
An Assessment of Safety Margins in Zircaloy Oxidation and Embrittlement Criteria for ECCS Acceptance

Prepared by R. E. Williford

Pacific Northwest Laboratory
Operated by
Battelle Memorial Institute

Prepared for
**U.S. Nuclear Regulatory
Commission**

NOTICE

This report was prepared as an account of work sponsored by an agency of the United States Government. Neither the United States Government nor any agency thereof, or any of their employees, makes any warranty, expressed or implied, or assumes any legal liability of responsibility for any third party's use, or the results of such use, of any information, apparatus, product or process disclosed in this report, or represents that its use by such third party would not infringe privately owned rights.

NOTICE

Availability of Reference Materials Cited in NRC Publications

Most documents cited in NRC publications will be available from one of the following sources:

1. The NRC Public Document Room, 1717 H Street, N.W.
Washington, DC 20555
2. The Superintendent of Documents, U.S. Government Printing Office, Post Office Box 37082,
Washington, DC 20013-7082
3. The National Technical Information Service, Springfield, VA 22161

Although the listing that follows represents the majority of documents cited in NRC publications, it is not intended to be exhaustive.

Referenced documents available for inspection and copying for a fee from the NRC Public Document Room include NRC correspondence and internal NRC memoranda; NRC Office of Inspection and Enforcement bulletins, circulars, information notices, inspection and investigation notices; Licensee Event Reports; vendor reports and correspondence; Commission papers; and applicant and licensee documents and correspondence.

The following documents in the NUREG series are available for purchase from the GPO Sales Program: formal NRC staff and contractor reports, NRC-sponsored conference proceedings, and NRC booklets and brochures. Also available are Regulatory Guides, NRC regulations in the *Code of Federal Regulations*, and *Nuclear Regulatory Commission Issuances*.

Documents available from the National Technical Information Service include NUREG series reports and technical reports prepared by other federal agencies and reports prepared by the Atomic Energy Commission, forerunner agency to the Nuclear Regulatory Commission.

Documents available from public and special technical libraries include all open literature items, such as books, journal and periodical articles, and transactions. *Federal Register* notices, federal and state legislation, and congressional reports can usually be obtained from these libraries.

Documents such as theses, dissertations, foreign reports and translations, and non-NRC conference proceedings are available for purchase from the organization sponsoring the publication cited.

Single copies of NRC draft reports are available free, to the extent of supply, upon written request to the Division of Technical Information and Document Control, U.S. Nuclear Regulatory Commission, Washington, DC 20555.

Copies of industry codes and standards used in a substantive manner in the NRC regulatory process are maintained at the NRC Library, 7920 Norfolk Avenue, Bethesda, Maryland, and are available there for reference use by the public. Codes and standards are usually copyrighted and may be purchased from the originating organization or, if they are American National Standards, from the American National Standards Institute, 1430 Broadway, New York, NY 10018.

An Assessment of Safety Margins in Zircaloy Oxidation and Embrittlement Criteria for ECCS Acceptance

Manuscript Completed: November 1985
Date Published: April 1986

Prepared by
R. E. Williford

Pacific Northwest Laboratory
Richland, WA 99352

Prepared for
Division of Accident Evaluation
Office of Nuclear Regulatory Research
U.S. Nuclear Regulatory Commission
Washington, D.C. 20555
NRC FIN B2277

ACKNOWLEDGMENTS

The author wishes to thank Dr. Robert Van Houten of the Fuel Systems Research Branch, USNRC, for his support of this work. Dr. John T. Prater and Mr. Galen M. Hesson of Pacific Northwest Laboratory are acknowledged for helpful discussions concerning oxidation rates and general LOCA characteristics. This work was performed by Pacific Northwest Laboratory under U.S. Department of Energy contract DE-AC06-76RLO 1830.



ABSTRACT

Current Emergency Core Cooling System (ECCS) Acceptance Criteria for light-water reactors include certain requirements pertaining to calculations of core performance during a Loss of Coolant Accident (LOCA). The Baker-Just correlation must be used to calculate Zircaloy-steam oxidation, calculated peak cladding temperatures (PCT) must not exceed 1204°C, and calculated oxidation must not exceed 17% equivalent cladding reacted (17% ECR). The minimum margin of safety was estimated for each of these criteria, based on research performed in the last decade. Margins were defined as the amounts of conservatism over and above the expected extreme values computed from the data base at specified confidence levels. The currently required Baker-Just oxidation correlation provides margins only over the 1100°C to 1500°C temperature range at the 95% confidence level. The PCT margins for thermal shock and handling failures are adequate at oxidation temperatures above 1204°C for 210 and 160 seconds, respectively, at the 95% confidence level. ECR thermal shock and handling margins at the 50% and 95% confidence levels, respectively, range between 2% and 7% ECR for the Baker-Just correlation, but vanish at temperatures between 1100°C and 1160°C for the best-estimate Cathcart-Pawel correlation. Use of the Cathcart-Pawel correlation for LOCA calculations can be justified at the 85% to 88% confidence level if cooling rate effects can be neglected.



CONTENTS

ACKNOWLEDGMENTS	iii
ABSTRACT	v
1.0 INTRODUCTION	1
2.0 DESCRIPTION OF RELEVANT PHENOMENA	3
3.0 THE DATA BASE IN 1973	9
4.0 RESEARCH PERFORMED SINCE 1974	13
4.1 ZIRCALOY-STEAM OXIDATION RATES	13
4.1.1 Recent Isothermal Oxidation Rate Data	13
4.1.2 Factors Affecting Oxidation Rates	22
4.1.3 Margins in the Oxidation Rate Data	34
4.2 EMBRITTLEMENT OF ZIRCALOY DURING OXIDATIONS	37
4.2.1 Recent Research Results	38
4.2.2 Margins in the PCT Criterion	43
4.2.3 Margins in the ECR Criterion	49
5.0 SUMMARY AND CONCLUSIONS	57
6.0 REFERENCES	59

FIGURES

1	Parabolic Oxidation Rate Constants for the Low Temperature Regime (1000-1500°C)	15
2	Oxide Growth Rate Constants for 1500-2300°C	19
3	Mean and Scatter of Low Temperature Oxidation Rate Constants	20
4	Mean and Scatter of High Temperature Oxidation Rate Data	21
5	Reduction of Rate Constants by Pre-Films	25
6	Factors Which Affect Oxidation Rate Constants (1000-1500°C)	26
7	Factors Which Affect Oxidation Rate Constants (1500-2300°C)	28
8	Oxidation Enhancement Factors Caused by Deformation	29
9	Enhancement Factor for Hydrogen Dilution	33
10	Basis for Oxidation Rate Constant Margin Assessment at Lower Temperatures	35
11	Percent Margin in Oxidation Rate Constants at Lower Temperatures	36
12	Percent Margin in the Oxidation Rate Constants at Higher Temperatures	37
13	Thermal Shock Failure Data: Laboratory Experiments	40
14	Thermal Shock Failure Data: In-Reactor Experiments	42
15	Handling Failure Data	44
16	PCT Margins for Thermal Shock	46
17	PCT Margins for Handling Failures	48
18	Estimated Minimum PCT Margins for Thermal Shock and Handling Failures at the 95% Confidence Level	50
19	Thermal Shock Failure Boundaries at the 95% Confidence Level	51
20	Thermal Shock and Handling Failure Boundaries at 50% and 95% Confidence Levels	53
21	Minimum ECR Margins for Thermal Shock and Handling Failures	55

TABLES

1	Parabolic Rate Constants for Total Oxygen Consumed (1000-1500°C)	14
2	Parabolic Rate Constants for Oxide Growth Rate (1500-2300°C)	18

1.0 INTRODUCTION

The postulated break of a pipeline in the primary core cooling system of a nuclear reactor can initiate a transient event called a Loss of Coolant Accident (LOCA). Such an event causes the reactor power to decrease very rapidly because the moderating coolant is lost from the core. However, some heat remains in the fuel rods as the fission products decay. Although the Emergency Core Cooling System (ECCS) replenishes the lost core coolant, there may be a short period of time before the fuel rods are again covered with cooling water. During this time, the decay heat would cause the fuel rods to undergo a temperature excursion, and the Zircaloy fuel rod cladding may reach temperatures of about 1000°C (1832°F) or possibly higher. Because the fuel rod internal pressures may be greater than the (external) coolant pressure in the core, the Zircaloy cladding may deform or swell to a configuration resembling localized ballooned regions along some of the rods. Some of the rods may subsequently also rupture, exposing the cladding internal surface to the steam atmosphere then prevailing in the core.

When the temperature of the Zircaloy cladding reaches about 1000°C, contact with the steam atmosphere causes significant oxidation to begin. The most oxidized portions of the cladding are those at the highest temperatures for the longest times, usually confined to a small region of the reactor core. Furthermore, the greatest oxidation occurs on the surfaces of the cladding, where brittle zirconium dioxide forms. Lesser oxidation occurs within the relatively protected inner regions across the cladding wall thickness. The more brittle layers of oxidized cladding cannot withstand significant loads without fracture, while the more ductile inner regions of the cladding may survive such loads if their oxygen content is not too high.

The loads referred to above are thermal shock loads that occur when the ECCS coolant reaches the cladding and begins to cool the core. The rapid cooling of the rods causes rapid thermal contractions, which are accompanied by axial restraint provided by the grid spacers, thus inducing axial loads on the oxygen embrittled cladding. Some circumferential loads are also induced by the internal thermal stresses in the cooling cladding, and bending stresses may be caused by cladding deformation/spacer grid interaction or by rod-to-rod interactions. When the cladding temperatures fall to 475-600°C, the efficiency of the coolant increases in a phenomenon called rewet. Maximum thermal shock loads then occur as the cooling rate increases, and may result in fracture or shattering of the oxygen embrittled portions of the Zircaloy cladding. These shattered portions could then fall toward the bottom of the core, resulting in a rubble pile that may be harder to cool than the original fuel rod geometry. The ballooning phenomenon described above has also been postulated to cause local hot spots because partial obstruction of the inter-rod coolant flow channels may impede coolant flow. These hot spots would naturally undergo greater oxidation and embrittlement: recent research has shown that this is generally not the case. Coolability-ballooning relationships are not the subject of the present report, which is focused on the oxidation embrittlement-shattering phenomenon.

Because of the potential safety-related consequences of a LOCA, the research arm of the U.S. Nuclear Regulatory Commission (NRC/RES, formerly the Atomic Energy Commission, AEC/RSR) developed criteria for the acceptance of ECCSs [1]. The criteria related to oxidation and embrittlement of the Zircaloy cladding took the form of maximum allowable limits for peak cladding temperatures and the amount of cladding oxidized that would be calculated to occur during a LOCA. These limits are (1) peak cladding temperatures (PCT) must not exceed 2200°F, and (2) the equivalent cladding reacted (ECR) must not exceed 17% of the cladding wall thickness. These limits were established in 1973. Because the NRC considered the data base concerning oxidation embrittlement to be insufficient at that time, the above PCT and ECR criteria were defined so as to incorporate conservatisms. The intent was to provide margins of safety that were sufficient to compensate for uncertainties in the data. In 1975, the American Physical Society completed a report [2] which outlined the deficiencies in the data base related to LOCA analyses. The AEC/RSR then redirected existing and implemented new research programs to respond to these needs. Similar or complementary research programs were initiated in other countries as well, such as the United Kingdom, the Federal Republic of Germany, and Japan. The results of this research were recently reviewed in [3].

The present report reviews PCT and ECR-related research performed in the last decade, and is focused on employing that research to better define the conservatisms (margins) in those criteria. Because the oxidation embrittlement behavior of Zircaloy cladding depends strongly on time and temperature, which in turn depend on the type of LOCA, cladding performance and failure behavior for Small Break LOCAs (SBLOCA), Large Break LOCAs (LBLOCA), and Severe Fuel Damage (SFD) scenarios will be delineated wherever possible.

2.0 DESCRIPTION OF RELEVANT PHENOMENA

This section consists of a brief qualitative description of the major physical phenomena which are active in the oxidation and embrittlement of Zircaloy cladding. The relationships between these physical processes and the nature of the LOCA are discussed wherever possible in order to provide perspective for the reader.

The most important factor controlling the rate of the Zircaloy-steam oxidation reaction is the temperature of the cladding. Because an important oxidation rate parameter increases exponentially with temperature, the oxidation rate becomes faster and faster as the temperature rises. The kinetics of this reaction are described in more detail in later paragraphs, while the focus of the immediately following paragraphs is on the relation of the oxidation rate to the type of LOCA and the approach to the 2200°F PCT and 17% ECR limits.

The rate of the oxidation reaction determines the time until the 17% ECR limit is reached, which in turn implies that the cladding is approaching the conditions necessary for failure during quench. The approach to cladding failure conditions is thus related to the time elapsed at high temperatures during a LOCA. For the purposes of this report, three basic classes of LOCAs are defined: the Large Break (LBLOCA), Small Break (SBLOCA), and the Severe Fuel Damage (SFD) scenario. These designations are terms frequently used to describe the limiting cases for a wide spectrum of possible scenarios. The LBLOCA is characterized by the complete rupture of a major pipeline supplying coolant to the core, which results in rapid expulsion of coolant from the core (blowdown), and a momentary temperature excursion of the fuel rods. This is followed by the refill stage, where the ECCS begins to refill the core with water, but the water has not yet reached the lower extremities of the fuel rods. Another temperature excursion begins, and the fuel rods may swell (balloon) and possibly rupture because the coolant (mostly steam at this stage of the LOCA) has been depressurized. If temperatures rise above 1000°C, cladding oxidation becomes significant. Further ECC injection brings the water level higher and begins to cover the fuel rods, and the cladding temperatures begin to fall as more heat is transferred to the coolant. When cladding temperatures fall to 450-600°C, cooling efficiency is increased (rewet), and the most severe thermal shock occurs as cooling rates then increase. The whole LBLOCA sequence is generally estimated to be completed in 100 to 200 seconds, during which time the majority, if not all, of the core will have been temporarily uncovered.

The SBLOCA is characterized by a less severe coolant pipeline break, where core coolant depressurization and complete expulsion (blowdown) may not occur. Rather, the smaller leak opening restricts coolant expulsion, and the coolant level in the core is reduced in part by blowdown. Consequently, only part of the core may be uncovered, so that only the upper portions of the fuel rods will undergo a significant temperature excursion and cladding oxidation. Cladding ballooning and rupture may not occur because the coolant may remain sufficiently pressurized. This pressurization can cause fuel-cladding contact, which ensures two-sided cladding oxidation above about 1100°C, where cladding

oxidation by the UO_2 fuel is roughly equivalent to that by steam. SBLOCAs are estimated to cover a wide range of time spans, depending on ECCS performance and leak size. However, the magnitude of the temperature excursion is generally expected to be less severe than in a LBLOCA.

The SFD scenario is frequently described as a LOCA with deficient ECCS performance. That is, the ECCS fluid is not supplied at sufficient rates to compensate for initial fluid loss and/or boildown, resulting in a more severe temperature excursion of the fuel rod cladding. Consequently, the cladding is presumed to become severely oxidized and overheated to the point of melting (about $1850^{\circ}C$), resulting in a loss of core geometry in the hottest regions of core. This overheat to melt syndrome is caused by the exothermic nature of the Zircaloy-steam reaction. As temperatures rise, heat is released by the reaction, which increases the temperature still further, thus accelerating the reaction. This exothermic behavior is one important reason why the $1204^{\circ}C$ ($2200^{\circ}F$) PCT limit was imposed. Other reasons are discussed in later paragraphs. Although significant oxidation and heat generation begin at about $1000^{\circ}C$ ($1800^{\circ}F$), the reaction and temperatures are generally considered to be controllable by the ECCS cooling capabilities until temperatures reach $1200^{\circ}C$. Beyond this temperature, the accelerating nature of the reaction presents increasing difficulties for the ECCS to reverse the temperature excursion and begin cooling the fuel rods. As cladding temperatures approach about $1427^{\circ}C$ ($2600^{\circ}F$), the temperature excursion is generally considered to be noncontrollable by the ECCS. The time span for the SFD scenario is generally longer than that for the type of LOCA from which the SFD event originated.

It should be noted that the above LOCA scenarios apply primarily to pressurized water reactors (PWRs), and that boiling water reactor (BWR) scenarios are somewhat different. However, only PWR LOCA descriptions are presented here because the largest power plants, and the largest number of plants, are PWRs. PWR LOCAs thus would present the greatest safety and economic impacts. This is reflected in the fact that the majority of related LOCA research has been performed for PWR systems. Descriptions of BWR LOCA scenarios may be found in [2].

It is apparent from the above descriptions of LOCA scenarios that a wide range of times and temperatures are of interest concerning Zircaloy-steam oxidation and embrittlement. Each scenario has a range of characteristic cladding temperature histories associated with it, and these temperatures are dominant in determining how quickly the cladding oxidation approaches conditions that render the Zircaloy susceptible to thermal shock failure. Each scenario will thus have a range of characteristic times before this condition is reached. The situation is further complicated by differences in cladding ballooning and rupture behavior, or by the extent of coolant depressurization, because these factors determine whether oxidation occurs predominantly on the outside of the cladding (in contact with the coolant) or on both sides.

Other synergistic mechanisms have also been proposed to be important in relation to Zircaloy oxidation and embrittlement during a LOCA. Two of the most important of these mechanisms are (1) the relation between cladding deformations (ballooning) and the cooling capabilities of the ECCS fluid, and

(2) the effects of the hydrogen evolved from the reaction in reducing the reaction rate itself (steam starvation). Cladding deformations have a number of effects on oxidation behavior. Ballooning reduces the inter-rod coolant passages and may cause local cladding hot spots if the coolant flow rate is low enough. The oxidation rate in these hot regions naturally increases with the temperature, reducing the time until the 17% ECR limit is reached. Deformations also reduce the cladding wall thickness, so that less metal needs to be oxidized before the above limit is reached, also reducing the allowable oxidation time. Deformations may also cause the oxide on the surface(s) of the cladding to crack, exposing portions of the metal deeper within the cladding wall to the oxidizing steam, accelerating the oxidation rate and reducing the allowable oxidation time. Although the latter is generally neglected, local heating near blocked zones and wall thinning may be important in assessing the conservatism in the 17% ECR criterion, along with the previously mentioned effect of cladding rupture in determining whether one or both sides of the cladding wall thickness undergo significant oxidation.

The steam starvation scenario originates from the presence of the hydrogen evolved from the Zircaloy-steam oxidation reaction. The excess hydrogen has been postulated to displace some of the steam at the Zircaloy surface, reducing the oxygen supply and the oxidation rate. Such a synergism would increase the time until the 17% ECR limit is reached. This may occur as the hydrogen accumulates near the top of the reactor core, or in the narrow fuel-cladding gap within the rod after cladding rupture permits steam ingress into the rod. Although the oxidation reaction would slow down, this may be compensated by embrittlement caused by hydrogen absorption by the Zircaloy. Recent research has shown that steam starvation generally does not occur significantly, and that hydrogen embrittlement effects are generally implicit in failure criteria because of the nature of the experiments conducted.

Although other synergisms such as the effect of oxygen content on Zircaloy deformation behavior (manifested in the rupture strain and coolant blockage correlations in Ref. 4) are also important, the main focus of this report concerns oxidation and embrittlement behavior. The following paragraphs therefore provide more detail about the physical phenomena active during these processes.

The Zircaloy-steam reaction is represented by the following molecular equation:



The reaction is exothermic, releasing 586 kJ/mole of zirconium reacted, along with four moles of hydrogen. At most temperatures of interest in a LOCA (above about 950°C) where the steam supply is unlimited and the oxide maintains integrity, the reaction is controlled by the rate of diffusion of oxygen anions through the anion deficient ZrO_2 film on the cladding surfaces. Such a diffusion controlled process is characterized by a parabolic rate law:

$$\frac{dW}{dt} = \frac{1}{2} \frac{\delta^2}{W} \quad (2)$$

where W can represent either the amount of reactant used or the amount of product formed, t is the oxidation time, and $\delta^2/2$ is the parabolic rate constant. Upon integration over time, Equation (2) becomes

$$W^2 = \delta^2 t + C \quad (3)$$

where C represents the initial amount of oxidation. The above rate constant depends on temperature T, as expressed by an Arrhenius relationship:

$$\delta^2/2 = A \exp(-Q/RT) \quad (4)$$

where A is the pre-exponential factor (a constant), Q is the activation energy, and R is the gas constant. The exponential effect of temperature on the oxidation rate can be readily seen from this equation.

The above parabolic rate equation represents the protective effects provided by the oxide layer acting as a diffusion barrier. At constant temperature, the rate of oxide growth decreases with time. However, other reaction rates are also possible. At lower temperatures and longer times typical of normal reactor operation, the oxide growth will begin via a cubic law [$W^3 = f(t)$], changing to a faster linear rate [$W = f(t)$] as the oxide develops cracks. At very high temperatures such as in an SFD scenario, phase transformations in the oxide may cause the oxidation rate to increase discontinuously as the diffusion barrier loses some of its protective nature. Although the parabolic rate equation is generally accepted as adequately describing Zircaloy-steam oxidation kinetics during LOCA conditions, there are also other limitations associated with the structure of oxidized cladding, as described below.

The high-temperature Zircaloy oxidation process results in the formation of three regions of differing properties across the cladding wall thickness: the oxide, a stabilized alpha layer and a beta layer. When the oxygen content of the Zircaloy exceeds about 26 percent by weight (wt%), zirconium dioxide forms. The ZrO_2 is a brittle ceramic even at high temperatures, and thus is considered to offer no effective resistance to fracture during thermal shock. At temperatures above about 810°C (for Zry-4), the hexagonal close packed Zircaloy (the alpha phase) begins to transform to a body centered cubic structure (the beta phase). However, oxygen that diffuses into the metal beneath the zirconia raises this transformation temperature (see for example Figure 4 of Ref. 5). The layer immediately beneath the oxide thus remains in the alpha phase, and is called the stabilized alpha layer. This layer is also quite brittle, and is generally considered to offer little or no resistance to fracture by thermal shock. Less oxygen diffuses into the central region of the cladding wall thickness, so that the transformation to the beta phase may be complete at temperatures above about 950-1000°C. If the oxygen content of the beta layer remains below certain limits, sufficient ductility is retained to offer resistance to fracture. Consequently, the beta layer is most important with respect to cladding thermal shock failures during LOCAs.

As the oxidation reaction progresses, the oxide and alpha layers grow in thickness, while the beta layer decreases. As temperature increases, the diffusion coefficient for the oxygen-beta Zircaloy system increases, as does the

solubility of oxygen in the beta phase. Consequently, the beta phase not only admits oxygen at a faster rate, it can also retain more. The effects of these phenomena in accelerating the embrittlement of the beta phase become significant at about 1204°C, which is another reason why the PCT limit was chosen as this value. The decrease in the beta phase thickness and its approach toward oxygen saturation also affect the apparent rate kinetics. The growth rates of the brittle oxide and alpha layers increase because there is no longer an infinite sink for the oxygen diffusing into the metal. However, total oxygen uptake decreases because the beta is no longer absorbing additional oxygen. The departure from parabolic kinetics via these mechanisms appears to become important near the 1204°C PCT limit for times longer than those expected for LBLOCAs, but may be important for SFD scenarios of longer duration at higher temperatures.

As the oxidized cladding begins to cool during the later stages of a LOCA, the beta phase is transformed to yet another phase with a complex microstructure, and is called the prior beta phase. During cooling, the solubility of oxygen in the beta phase decreases. It is the nature of the material for the oxygen to then redistribute into precipitates called alpha-incursions within the prior beta phase. This produces an inhomogeneous microstructure with brittle, high oxygen content platelets embedded in a more ductile matrix. The extent to which this occurs depends on the initial oxygen content in the beta phase before cooling and on the cooling rate. At lower oxygen contents and slower cooling rates, there is sufficient time for this redistribution to occur, and sufficient sites for the nucleation of alpha incursions, so that the resulting microstructure may resemble a particulate composite. This version of the prior beta phase is still somewhat capable of surviving thermal shocks without fracture because the oxygen depleted zones in the prior beta region retain significant ductility. However, as the oxygen content and cooling rate increase, the available time and number of incursion nucleation sites for oxygen redistribution decrease, resulting in a more uniformly brittle prior beta phase that is more susceptible to fracture. It is tempting to conclude that slower cooling rates are beneficial. However, this takes additional time during which the Zircaloy is further oxidized, so that the resulting embrittlement depends on the LOCA history in a complex manner.

The failure susceptibility of oxidation-embrittled Zircaloy cladding has been investigated over a wide range of temperatures, and various failure criteria have been developed in addition to the 1204°C PCT and 17% ECR limits. The data developed in the last decade will be reviewed in the following sections, beginning with a summary of the state-of-the-technology as it existed when the present criteria were implemented in 1973. This is intended to provide the reader with perspective concerning the substantial amount of research performed and scientific understanding gained with the objective of defining LOCA ECCS Acceptance Criteria which are sufficient to ensure public safety. In doing so, this report will attempt to measure the above by comparison of the uncertainties in the data base to the conservatism in the criteria, in essence assigning numbers to the "margins" of conservatism in the criteria and to the importance of those margins.

3.0 THE DATA BASE IN 1973

There were essentially two important data bases that were used in 1972-73 to define the PCT and ECR limits of the ECCS Acceptance Criteria. The first was the data base concerning Zircaloy-steam oxidation rates at various temperatures, and the second concerned the thermal shock performance of oxidation embrittled cladding. The oxidation rate data base was reviewed by M. L. Picklesimer, formerly of the USNRC, in early 1982, while the second was reviewed by Chung and Kassner [5] in 1980. The paragraphs below are brief summaries of the above reviews.

Data concerning Zircaloy-steam oxidation rates were rather sparse at the time of the ECCS hearings in 1972-73. Lemmon [6] had conducted experiments using standard ring specimens exposed to steam at temperatures above about 850°C in a tube furnace. The thermocouples were in intimate contact with the samples, and oxidation rates were calculated from the weight gains of the specimens. Bostrom [7] had conducted experiments in high temperature water. Baker and Just [8] used the above data plus their own data at nominally the melting point of zirconium (1850°C) to compute an oxidation rate curve spanning the temperature range from about 500°C to about 1850°C. Picklesimer has outlined the deficiencies in the Baker-Just data base as follows:

1. Oxidation rates were determined from the hydrogen evolved from short wire specimens immersed in water and electrically heated by condenser bank discharge;
2. Specimen temperatures were computed from condenser bank storage energies, wire dimensions, and an assumed electrical resistivity-temperature relation for zirconium;
3. The appearance of small droplets of zirconium-ZrO₂ in the test chamber were taken to represent that oxidation occurred at the zirconium melting point;
4. However, self-heating of the specimen via the exothermic nature of the reaction was ignored.

Additionally, the Baker-Just correlation is an extrapolation from the low-temperature data of Lemmon and Bostrom to the melting point data of Baker and Just, with no confirming data points in the intermediate temperature ranges. It is generally argued that the Baker-Just correlation, currently required in the criteria, is substantially conservative.

Hobson and Rittenhouse [9] conducted experiments related to the embrittlement characteristics of Zircaloy. Long tubular specimens of standard Zircaloy cladding were exposed to steam at various times and temperatures in a tube furnace. Sections cut from the tubes were subjected to metallographic analyses to determine the thicknesses of the reaction layers, along with mechanical properties. These data were analyzed by Pawel [10,11] for comparison to the Baker-Just rate equation, and the results of this analysis were available in early

1973. Although later analyses showed Pawel's results to be in good agreement with current (1985) best-estimate oxidation rate equations, Pawel's results were apparently given lesser weight during the hearings. The NRC (AEC in 1973) instead chose a different approach with two features: (1) the Baker-Just oxidation rate equation was chosen as a part of the criteria because it conservatively bounded all other data known at that time, thus incorporating a safety factor to compensate for uncertainties in the data base; (2) the AEC directed that further research be performed to better define the oxidation rate equation [12].

The second data base contributing to the development of the criteria concerned the thermal shock performance of oxidation embrittled Zircaloy cladding. One intent of these experiments was to define an easily usable oxidation parameter that was related to the cladding metallurgical state at which failure by thermal shock loads during quench occurred. One such parameter is the equivalent cladding reacted (ECR), or the fraction of the cladding wall thickness that would be converted to oxide if all the oxygen absorbed by and reacted with the Zircaloy were converted to stoichiometric ZrO_2 . Another such parameter is the fraction of the wall thickness that remains in the beta phase (F_w). Research in the last decade has indicated that the stipulation of a thickness and the maximum amount of oxygen allowed in the beta phase can yield more refined criteria with possibly less uncertainty. This is probably due to the fact that two independent parameters determine oxidation state: time and temperature. However, this was not yet clear during the 1972-73 hearings, and the accepted practice at that time was to employ a single scalar parameter to describe the oxidized metallurgical state of the cladding. Therefore, the embrittlement data base is discussed below in terms of these single parameters.

Hesson et al. [13] induction-heated Zircaloy cladding containing UO_2 pellets in flowing steam for various times and temperatures, and quenched the samples in room temperature water. The samples did not balloon or rupture, and only single-sided oxidation occurred. Reaction kinetics were determined via hydrogen evolution measurements, and oxide layer thicknesses were determined via metallographic analysis. It was found that cladding heated to temperatures $< 1657^\circ C$ with total oxidation $< 17\%$ ECR survived thermal shock upon quenching, but that cladding heated to temperatures above about $1567^\circ C$ with $ECR \geq 18.4\%$ failed either during quench or during subsequent handling.

Thermal shock tests were conducted by Duncan and Leonard [14] on electrically heated, full scale, simulated BWR 7x7 bundles, which also did not balloon or rupture. Thermal histories were controlled by top spray cooling to simulate decay heat effects during cooling. A limited number of metallographic analyses showed that the rods remained intact after rapid cooling if temperatures were less than about $1327^\circ C$ and the total oxidation was less than about 16.4% ECR. Scatena's [15] single-rod tests were also electrically heated, but quench was achieved by bottom flooding with water. There was also no ballooning or rupture in these experiments. Twenty four tubes oxidized at temperatures between about $827^\circ C$ and $1497^\circ C$ with resulting ECRs less than about 13% remained intact after quenching. One tube oxidized at $1590^\circ C$, with $ECR = 17.6\%$, failed upon quenching.

It was apparent from the above data that the failure boundary was reasonably well defined by 17% ECR. Thus, 17% ECR was chosen as the limiting measure of oxidation for the ECCS acceptance criteria. However, data were relatively sparse at lower temperatures representative of the majority of LOCA scenarios. Additionally, other data indicated that the 17% ECR limit alone appeared to be insufficient to compensate for uncertainties concerning thermal shock failures after higher temperature oxidation. These data include the ring loading experiments of Meservey and Herzel [16], and more importantly the ring loading experiments of Hobson and Rittenhouse [9] and Hobson [17]. In the latter two references, correlations were developed describing the "zero ductility" state of oxidized ring specimens during impact compression tests at room temperature as functions of the F_w parameter for specimens oxidized at 927°C to 1372°C and quenched in water. A similar correlation for a slow compression rate (0.0423 mm/sec) was valid only below 1204°C (2200°F), while specimens oxidized at temperatures above 1315°C had unexpectedly low ductility. It was clear from these data that embrittlement was not simply a function of ECR or of F_w , but also depended on the amount and distribution of oxygen in the beta layer [9,17]. Because these factors depend on the beta Zircaloy-oxygen diffusion coefficient [18,19] and on the terminal solubility of oxygen in the beta phase [20], which both depend exponentially on temperature, a maximum allowable temperature of 1204°C (2200°F) was also specified as part of the ECCS Acceptance Criteria. Although Pawel [10] had proposed criteria based on 95% maximum saturation of the beta phase (0.7 wt% below 1247°C), the maximum PCT limit of 1204°C was chosen because of the complexities and uncertainties involved in computing oxygen distributions for various LOCA scenarios with non-steady state temperature histories.

The criteria were adopted by the AEC on December 28, 1973 [12]. The PCT and ECR criteria are repeated below:

- 1) Peak Cladding Temperature. The calculated maximum fuel-element cladding temperature shall not exceed 1204°C (2200°F).
- 2) Maximum Cladding Oxidation. The calculated total oxidation of the cladding shall nowhere exceed 0.17 times the total cladding thickness before oxidation. As used in this subparagraph, the total oxidation means the total thickness of cladding metal that would be locally converted to oxide if all the oxygen absorbed and reacted with the cladding locally were converted to stoichiometric zirconium dioxide. If cladding rupture is calculated to occur, the inside surfaces of the cladding shall be included in the oxidation, beginning at the calculated time of rupture. Cladding thickness before oxidation means the radial distance from the inside to outside of the cladding, after any calculated rupture or swelling has occurred but before significant oxidation. Where the calculated conditions of transient pressure and temperature lead to a prediction of cladding swelling, with or without cladding rupture, the oxidized cladding thickness shall be defined as the cladding cross-sectional area, taken at a horizontal plane at the elevation of rupture, if it occurs, or at the elevation of the

highest cladding temperature if no rupture is calculated to occur, divided by the average circumference at that elevation. For ruptured cladding the circumference does not include the rupture opening.

- 3) Maximum Hydrogen Generation. The calculated total amount of hydrogen generated from the chemical reaction of the cladding with water or steam shall not exceed 0.01 times the hypothetical amount that would be generated if all the metal in the cladding cylinders surrounding the fuel, excluding the cladding surrounding the plenum volume, were to react.
- 4) Coolable Geometry. Calculated changes in the core geometry shall be such that the core remains amenable to cooling.
- 5) Long-term Cooling. After any calculated successful initial operation of the ECCS, the calculated core temperature shall be maintained at an acceptably low value and decay heat removed for the extended period of time required by the long-lived radioactivity remaining in the core.

The inclusion of the requirement to consider the effects of cladding deformation (ballooning) and rupture on the calculated oxidation raised further questions concerning the adequacy and uncertainties of the data base. Consequently, new research was initiated to remedy this situation. The following sections include summaries of the work performed in the last decade.

4.0 RESEARCH PERFORMED SINCE 1974

A substantial amount of research has been performed in the last decade in relation to Zircaloy-steam oxidation and embrittlement. The influence of these phenomena on fuel rod performance and survivability during a LOCA has been of international importance, and investigations have been conducted in the United States, United Kingdom, Japan, West Germany and Canada. The amount and quality of results produced has subsequently made it possible to quantitatively estimate the conservatisms, or margins of safety, in the present LOCA ECCS Acceptance Criteria, and to compare these margins to the uncertainties in the data base as it now exists. Such is the purpose of this report.

Research directly related to the 1204°F PCT and 17% ECR criteria falls into two broad categories: Zircaloy-steam oxidation rates and oxidation embrittlement-shock failure data. The first category determines the amount of oxidation occurring at a given time-temperature combination for a given LOCA scenario and in essence determines the amount of embrittlement. The second category combines embrittlement with the loading conditions to address the main objective of the criteria, which is the prevention of cladding failures during a LOCA. Research performed in both categories is reviewed below, and an attempt is made to quantify and compare uncertainties and safety margins. The text follows much the same approach as other recent reviews, such as [3].

4.1 ZIRCALOY-STEAM OXIDATION RATES

4.1.1 Recent Isothermal Oxidation Rate Data

1000-1500°C

Biederman et al. [21] oxidized Zircaloy-4 tube specimens in steam over the range 871-1482°C. The experimental apparatus employed was called a "Gleeble", which used electrical resistance to heat the tubes. Steam flowed into the Gleeble through the sample tube itself, becoming essentially stagnant with respect to oxidation of the outer surface of the Zircaloy tube. Because of heat loss from the tube to the apparatus, temperature gradients across the oxide layer on the outer surface of the tube could be about 40°C per 100 microns of oxide thickness. Although temperatures were measured by thermocouples seated in notches or grooves in the outer wall of the cladding, questions have been raised concerning the accuracy and calibration of temperature measurements. The extent of reaction was measured by weight gains and by measurements of the thicknesses of the oxidized phases, and showed the reaction to follow a parabolic rate law above the alpha/beta transition temperature. The Arrhenius relation for the total oxygen consumption is shown in Table 1 and Figure 1. Total oxygen consumption is used to compute the Equivalent Cladding Reacted (ECR) in the ECCS Acceptance Criteria. Other rate constants for hydrogen evolution and Zircaloy consumed may be seen in Table 1 of [3]. Picklesimer has reviewed Biederman's data and has developed a rate constant which is much closer to that of Cathcart and Pawel [22], discussed below.

TABLE 1. Parabolic Rate Constants for Total Oxygen Consumed (1000-1500°C)

$$\delta^2/2 = A \exp(-Q/RT) \quad (\text{gm O}_2/\text{cm}^2)^2/\text{sec}$$

Curve No. (Figure 1)	Source [ref.]	Date	Range (°C)	A	Q (cal/mole)
1	Biederman [21]	1977	980-1480	0.0191	33,370
2	Cathcart-Pawel [22]	1977	1000-1500	0.1811	39,940
3	Westerman [23]	1977	970-1250	0.0321	34,700
4	Biederman [24] ^(a)	1978	650-816	5.73×10^{-4}	27,340
5	Kawasaki et al. [25,26]	1978	1000-1330	0.234	40,710
5a	Komatsu [25]	1978	950-1300	0.1094	38,000
6	Urbanic-Heidrick [27]	1978 1978 ^(a)	1050-1580 1580-1850	0.0182 0.0541	33,420 33,004
7	Leistikow, et al. [28]	1978	1000-1300	0.262	41,653
8	Brown-Healey [29]	1980	1000-1200 1200-1400	0.1028 0.2238	38,984 41,627
9	Hobson-Pawel [9,10]	1973	962-1406	0.1553	39,291
10	Baker-Just [8] ^(a)	1962	500-1852	2.049	45,500

(a) Not included in averages.

Cathcart and Pawel [22] heated 1-2 cm long standard tube sections in a quartz-elliptical furnace with a very low velocity of steam at atmospheric pressure over the temperature range 900-1500°C. Temperatures were measured "with great precision" by thermocouples welded to the inner surfaces of the samples, which were sealed to permit oxidation of the outer surface only. Parabolic oxidation rate constants were determined by measurement of weight gains and metallography. The rate constant for the total oxygen consumed appears in Table 1 and Figure 1. Note that these rate constants are valid only above 1000°C, because the reaction exhibited a cubic growth rate at lower temperatures. This is associated with an oxide phase change from dense monoclinic to a porous mixed monoclinic/tetragonal phase.

Westerman and Hesson [23] found parabolic reaction rates over the temperature range 973-1251°C using an induction furnace with steam flowing at 7.5 gm/min. The extent of reaction was measured by hydrogen evolution and by metallography of oxidized phase widths. The rate constant for consumed oxygen

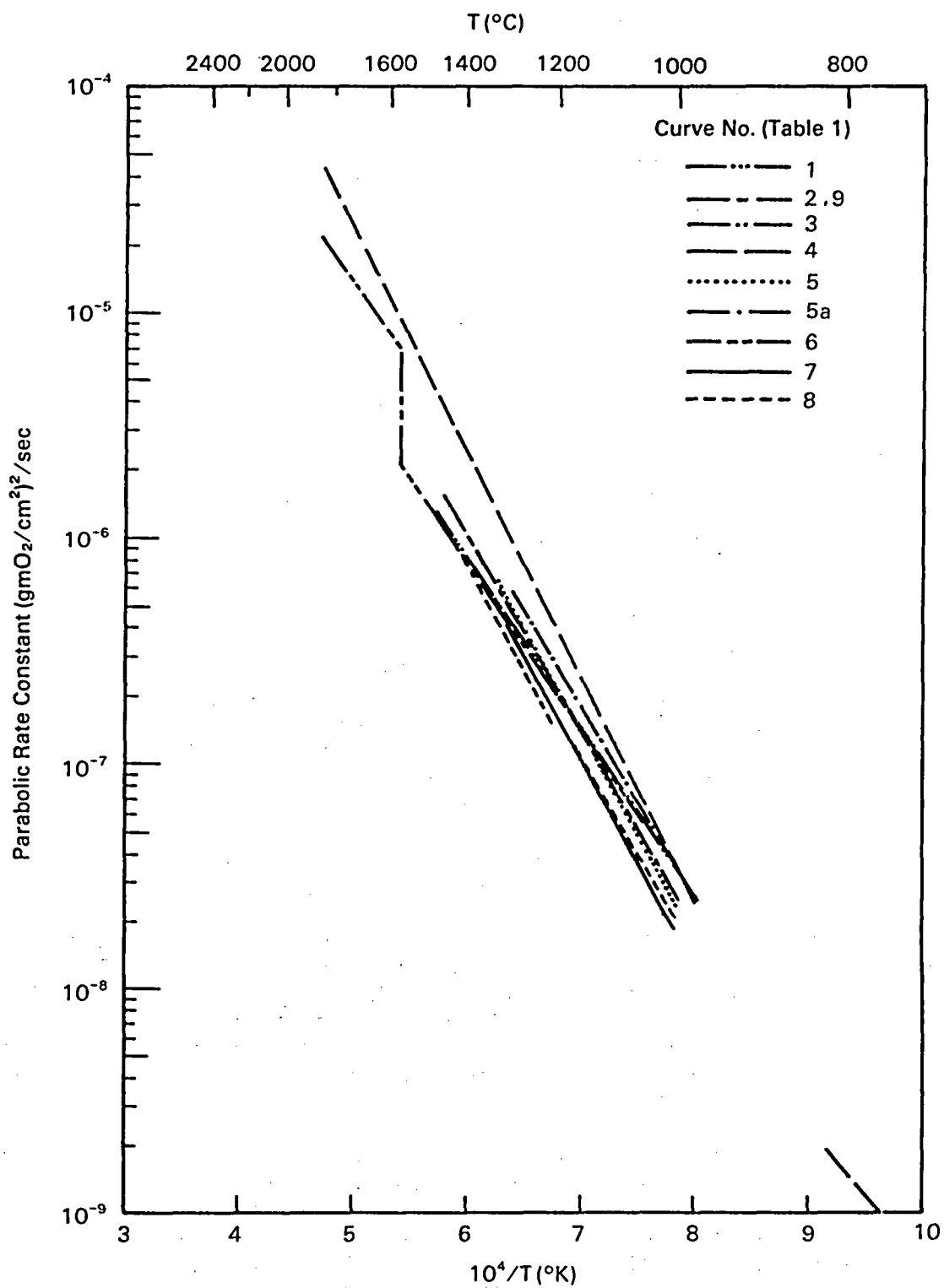


FIGURE 1. Parabolic Oxidation Rate Constants for the Low Temperature Regime (1000-1500°C)

is shown in Table 1 and Figure 1. It is also of note that hydrogen absorption was measured to be 220-250 ppm in these experiments, amounts "much greater than the usual 20-30 ppm."

Biederman [24] investigated Zircaloy-steam reaction rates at lower temperatures ranging from 650-980°C. Reaction rates were found not to conform to an Arrhenius relationship over the mixed alpha/beta range of the Zircaloy (871-980°C). However, the parabolic rate constants shown in Table 1 did obey such a relation over the temperature range 650-816°C, although the rate constant so plotted in Figure 1 can obviously not be directly extrapolated from the higher temperature data in [21].

Kawasaki et al. [25,26] exposed both inner and outer surfaces of 15 mm long Zircaloy tube specimens to steam flowing at 0.4 gm/cm² min in a horizontal tube furnace. Sample temperatures were measured by thermocouples attached to the outer surface and placed near the inner surface of the tube segments. The specimens required 10 to 20 seconds to reach test temperatures, and were cooled by withdrawal from the furnace into laboratory air. Oxidation was measured by weight gains and metallographic (phase thickness) analyses, but were not corrected for oxidation occurring during heatup or cooldown. The resulting parabolic rate constants were found to be valid only for temperatures of 1000-1330°C (Table 1). The reaction did not follow parabolic kinetics at 800 and 950°C. The results in Figure 1 are similar to others despite the difference in experimental methods. Kawasaki [25] also shows other data by Ikeda and by Komatsu, but only in graphical form. Ikeda's data closely matches that of Kawasaki and of Cathcart-Pawel. However, Komatsu's data show slightly higher oxygen consumption rates, and are included in order to assess margins in conservatism. It should be noted that the pre-exponential rate constant in Table 1 was interpreted graphically from Komatsu's Figure 2a. Also included are results of the analysis of the Hobson-Rittenhouse data [9] by Pawel [10], which are seen to be very similar to the Cathcart-Pawel results [22].

Urbanic and Heidrick [27] oxidized Zircaloy-2 and -4 in unlimited steam in an induction furnace over the temperature range 1150-1850°C. Measurements of weight gains, hydrogen evolution, and oxide phase thicknesses showed parabolic oxidation rates to dominate over the entire temperature range. However, the oxide morphology changed from tetragonal to cubic at about 1580°C, and two different rates were observed above and below this temperature. Above 1580°C, the cubic phase is much more porous, and the oxygen consumption is considerably faster, as shown in Table 1 and Figure 1. It should be noted that these experiments are currently being repeated, but referencable results were not available at this writing.

Leistikow et al. [28] used both tube furnaces and induction heating in low steam flows (1 mg/sec) to study the Zircaloy-steam reaction over the temperature range 700-1300°C. All specimens were oxidized on both inside and outside tube surfaces, and temperatures were measured by thermocouples. Oxidation rates were measured by weight changes and metallographic analyses of oxidation layer thicknesses. The rate kinetics were parabolic above 900°C, but appeared to be cubic below this temperature. The parabolic rate constants for the temperature range 1000-1300°C are shown in Table 1 and Figure 1. Unpublished work

on oxidation rates during transient heating by Sagat et al., of AECL at Chalk River is reported [3] to be in close agreement with the isothermal studies of [28].

Brown and Healey [29] oxidized Zircaloy specimens in steam in a tube furnace over the temperature range 1000-1400°C. They found different behavior above and below 1200°C, caused by the formation of a duplex oxide film above that temperature. The formation of the duplex film is caused by the precipitation of tin-rich particles between the two oxide layers, an occurrence reported by many others. The parabolic rate constants for the two temperature regimes are shown in Table 1 and plotted in Figure 1.

1500-2300°C

The above data are generally applicable over the temperature range of 1000-1500°C, which encompasses all reasonable conditions anticipated for the LBLOCA and SBLOCA. However, the SFD scenario is postulated to reach even higher temperatures. Data applicable to the regime from 1500 to 2300°C have been produced in the last several years, and are reviewed in the following paragraphs.

Results are most often reported in terms of oxide growth rates (cm/sec^2) in the higher temperature ranges because experimental determination of oxide thicknesses is a more reliable measurement than oxygen consumption for the relatively short times required for the oxidation to near complete consumption of the Zircaloy. At higher temperatures, the accuracy of experimentally determined Zircaloy-steam reaction rate equations is affected by the exothermic reaction heat. This phenomenon causes temperature gradients to occur across the oxide film, and the determination of the appropriate temperature of the reaction is often a difficult task. This is also compounded by phase changes in the oxide itself. Between 1500 and 1600°C, the oxide changes from tetragonal to cubic in structure, and the decrease in density permits oxygen to diffuse to the metal at a faster rate. The result is an apparent discontinuous rise in the oxidation rate.

Urbanic and Heidrick [27] reported that the phase-induced change in the parabolic rate constant appeared to occur at about 1580°C, and reported the rate constants shown in Table 2 and Figure 2. Chung and Thomas [30] observed the rate change at about the same temperature, but apparently reported only the data rather than computed rate constants. Although Chung and Thomas also performed experiments at lower temperatures, only the data above 1580°C are shown in Figure 2. It should be noted that the data points shown connected by a line in Figure 2 were interpreted from Figure 5 of [3]. Aly [31] and Leistikow et al. [32] performed tests on Zircaloy tube sections in flowing steam over the temperature range of 1300-1600°C, finding faster parabolic reaction rates at 1550 and 1600°C accompanied by a dual-layered oxide. The inner layer was thought to have been a cubic phase containing alpha-Zircaloy precipitates.

Most recently, Prater and Courtright [33] have performed experiments using laser heated disc specimens and measured sample temperatures with a two-color pyrometer. Calibrations were carefully performed and temperature gradients

TABLE 2. Parabolic Rate Constants for Oxide Growth Rate (1500-2300°C)

$$\delta = A \exp(-Q/RT) \quad (\text{cm/sec}^{1/2})$$

Curve No. (Figure 2)	Source [ref.]	Date	Range (°C)	A	Q (cal/mol)
1	Urbanic-Heidrick [27]	1978	1580-1850	0.144	15,910
2	Chung-Thomas [30]	1982	1600-1700	Data Points Only	
3	Leistikow [32]	1983	1500-1600	Data Points Only ^(a)	
4	Prater-Courtright [33]	1985	1510-2400	5.46	28,235
5	Baker-Just [8]	1962	500-1852	2.3455	26,599

(a) Not included in mean.

across the sample were accounted for, resulting in accuracies of $\pm 15^\circ\text{C}$ over the range of 1300-2400°C. They observed the phase induced oxidation rate change to occur at 1510°C, with no additional rate change occurring upon Zircaloy melting. The resulting parabolic rate constant for oxide growth is shown in Table 2 and Figure 2, and is reported to have an uncertainty of $\pm 35\%$.

Scatter in the Data Base

In preparation for comparisons to be made in the next section of this report, the means and standard deviations (at the 2σ or 95% confidence level) were computed for both the low and high temperature oxidation rate data bases. The results are shown in Figures 3 and 4, and were computed from the correlations in Tables 1 and 2. It is important to note that the scatter for each individual correlation was ignored, and that the inclusion of such scatter would increase the widths of the shaded regions in Figures 3 and 4. Computations for the low temperature data were straightforward, but deficiencies in the high temperature data base resulted in a rather large standard deviation. This is evidenced by the inability to compute a lower bound at the 2σ limit in Figure 4. The data of Chung and Thomas [30] were included by fitting a short curve to the three data points in Figure 2, but Leistikow's [32] data were considered to be too ill-conditioned for inclusion. Note also that the Baker-Just relation was included in computing the mean and standard deviation in Figure 4. Future revisions of the Urbanic-Heidrick data [27] may produce results closer to those of Prater-Courtright [33], thus reducing the scatter in Figures 3 and 4.

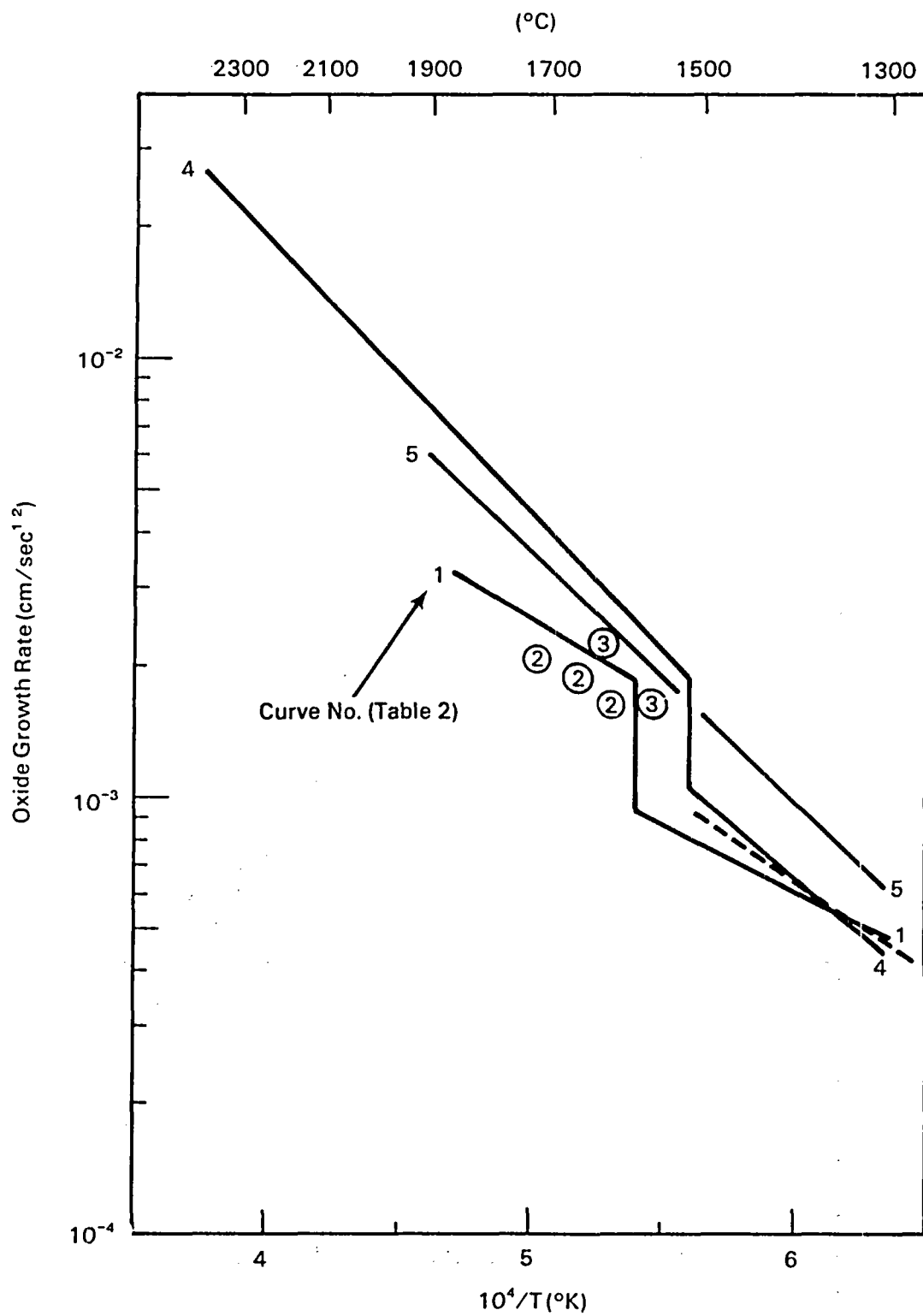


FIGURE 2. Oxide Growth Rate Constants for 1500-2300°C

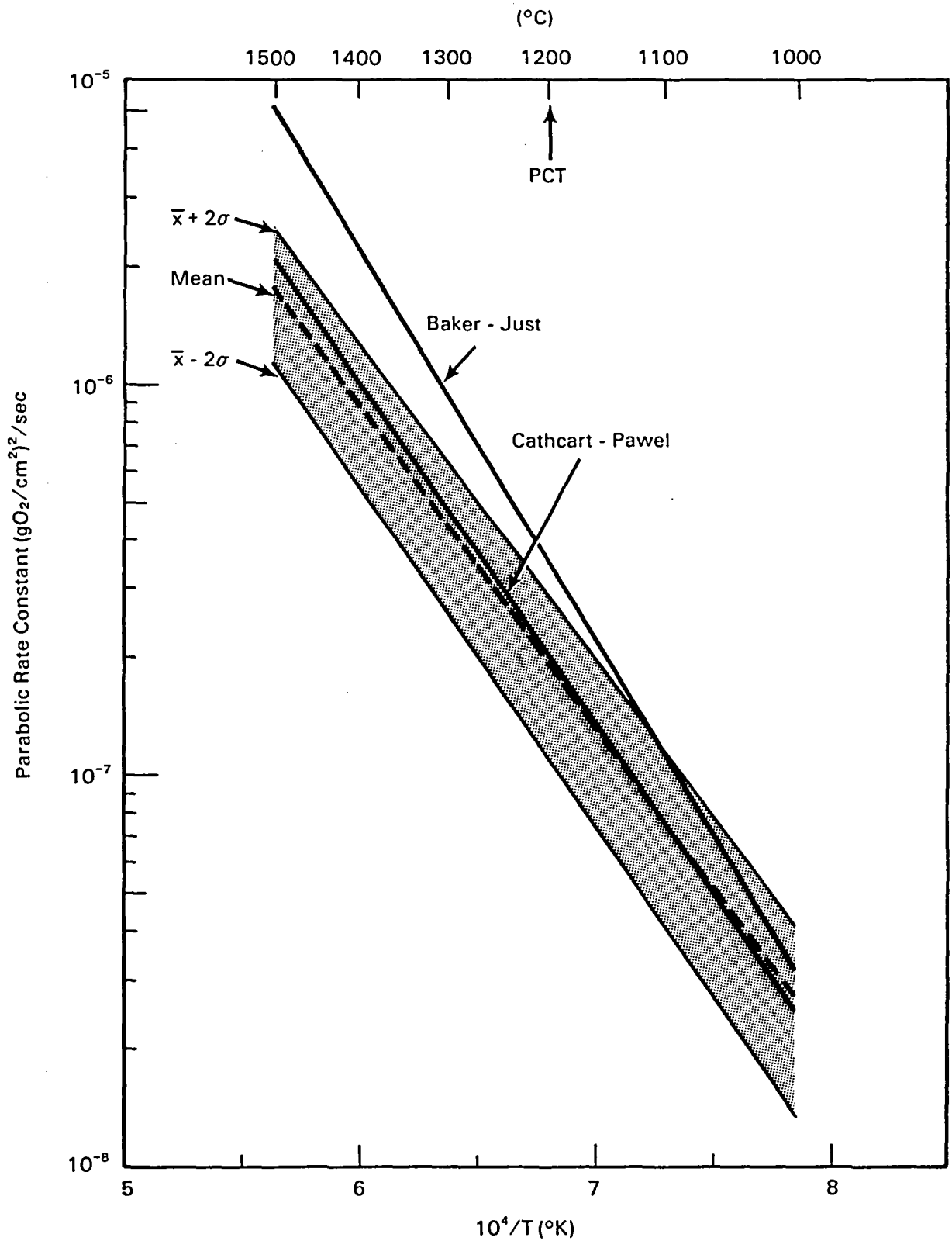


FIGURE 3. Mean and Scatter of Low Temperature Oxidation Rate Constants

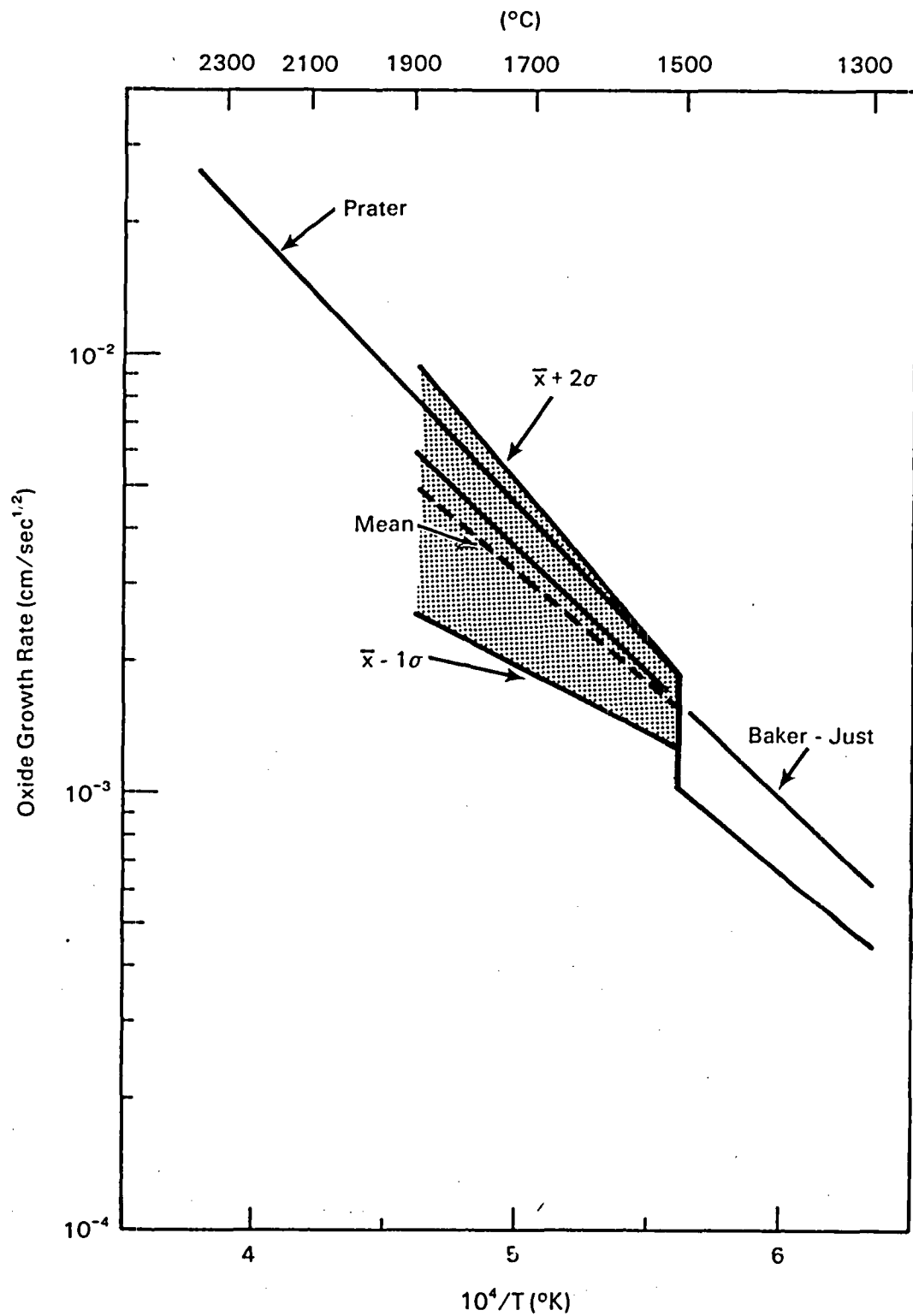


FIGURE 4. Mean and Scatter of High Temperature Oxidation Rate Data

4.1.2 Factors Affecting Oxidation Rates

A number of factors may affect the oxidation rate of the Zircaloy-steam reaction. Phenomena such as "breakaway" oxidation, caused by changes in the oxide film morphology, or deformation, which causes oxide cracking, may result in an increase in the apparent oxidation rate because the accessibility of oxygen to the metal is increased. Conversely, factors such as hydrogen dilution of the steam at the Zircaloy surface have been postulated to slow the oxidation rate because of "steam starvation", which reduces accessibility. Research performed in the last decade to assess the effects of such phenomena is reviewed in the following paragraphs, and an attempt will be made in a subsequent subsection to incorporate these phenomena into the assessments of the margins of conservatism in the current ECCS Acceptance Criteria.

Breakaway Oxidation

Breakaway is a term employed to describe an apparent increase in oxidation rate which is not predicted by thermal arguments alone. In particular, an oxide phase change may result in a more porous diffusion barrier for the influx of oxygen to the underlying metal. This in turn increases the oxygen supply rate and thus the oxidation rate itself. Several observations of breakaway behavior have been mentioned in previous sections of this report, and the purpose of this section is to review those effects on oxidation rate uncertainties during a LOCA.

At temperatures below about 800-850°C, the oxide remains in the tetragonal phase, and increases in oxidation kinetics from cubic to linear occur if times are sufficiently long [32]. Such a transition is said to be caused by oxide cracking. As the oxide grows, compressive stresses are developed because of the volumetric expansion (about 56%) associated with the uptake of oxygen to form the oxide from the metal. The compressive stresses are greatest in a direction parallel to the tube surface. When stresses reach a sufficient level, oxide buckling may occur, leaving small localized, lenticular-like voids also oriented roughly parallel to the tube surface. This occurs about every 2-3 microns of oxide thickness. The bending associated with the buckling may in turn introduce radial cracks in the oxide layers. The end result is that the effective porosity of the oxide is great enough to nearly eliminate the diffusion barrier characteristics of the oxide, and the oxidation rate becomes linearly dependent on the oxygen supply. An alternative mechanism is that stresses in the oxide film promote recrystallization and pore generation, which in turn enhances cracking [34].

Between temperatures of about 850 to 980°C, the Zircaloy undergoes a phase transformation from alpha to beta, while oxidation kinetics change from cubic to parabolic. Although breakaway to linear kinetics is rare, Leistikow et al. [32] observed it under transient heating conditions if oxide thicknesses were greater than an apparent critical value.

The oxide undergoes a phase transformation from tetragonal to monoclinic over the temperature range of about 950 to 1050°C. Grain coarsening, pore generation, and possible oxide cracking occur and may again cause oxidation

kinetics to change from cubic to linear [32]. The pores also cause the scalloped oxide/metal interface to develop at this stage by locally retarding oxide growth [35]. Data in this temperature range are frequently excluded from determination of rate constants in the higher temperature ranges.

Between the temperatures of about 1050°C to about 1500-1600°C, oxidation rate kinetics are almost exclusively parabolic. The rate constants for this temperature range, which is most important for LOCA analyses, were plotted in Figure 1.

At about 1500-1600°C, the oxide phase changes from monoclinic to cubic, and the increased oxide porosity causes an apparent step increase in the parabolic rate constants [33]. The rate constants remain parabolic up to about 2300°C, and are not affected by the melting of the Zircaloy at about 1850°C [33].

It is apparent from the above discussion that breakaway effects do not introduce any direct addition to uncertainties in oxidation rate data because this phenomenon does not occur over the range of temperatures of interest for LOCA analyses (>1000°C). Below this temperature, oxidation rates are generally so slow that the 17% ECR limit would not be expected to be approached. However, the effects of oxide films formed during normal reactor operation prior to a LOCA have been postulated to cause apparent changes in the parabolic rate constants, as discussed below.

Effects of Oxidation Prior to a LOCA

During normal reactor operation, the oxidation kinetics will be cubic for the first 100-500 days, until the oxide reaches a thickness of 2-5 microns, where transition to linear rates occur as described above. The oxide thicknesses at end of life (about 30 GWd/MTM) may range between 5 and 50 microns. This "initial" oxide (prior to the LOCA) will reduce the heat transfer characteristics of the fuel rod and will thus lead to slightly higher temperatures at the oxide/metal interface during the LOCA. This in turn may result in apparently faster rate kinetics. Although this initial oxide was formed in a radiation field, no effects are expected under LOCA conditions because the radiation damage anneals out at 400-450°C via thermally activated recovery processes [34,36,37].

Leistikow et al. [28] pre-formed oxides up to 50 microns thick at 350-600°C prior to subsequent testing at 1000 and 1200°C. They concluded that the preformed oxides were generally protective if subsequent temperatures remained below 1204°C (the current PCT limit). Quantitative evaluation of this protective effect is apparently not available. At higher temperatures, the tetragonal phase of the oxide formed and the protective effects decreased. Leistikow et al. [32] also pre-formed oxides up to 30 microns thick at 400-800°C, subsequently exposing the samples to transient oxidation conditions. They concluded that the effects of the initial oxide layer on subsequent kinetics were not systematic and did not provide an adequate data base for modeling the phenomenon.

Biederman [24] pre-formed 5 and 10 micron oxide films at 871°C and subsequently oxidized the samples at 980-1315°C. Although slower rate kinetics were reported, the analysis has been questioned by Mann et al. [3]. The rate reduction for 10 μ films ranged between 52% at 982°C to 23% at 1316°C, while the rate reduction for the 5 micron prefilm ranged between 9% at 982°C to about zero at 1204°C. Kawasaki et al. [25] found a protective effect for one micron thick initial oxides formed at 300°C and subsequently oxidized at 900 and 950°C for up to 50 mins, the weight gain being reduced by about 25-10%, decreasing as time increased. At higher temperatures, the preoxidation was not effective.

Mann, et al. [3] have commented on the unpublished work of Inglesias (AECL) as follows....Although protective effects of preoxides have been claimed for temperatures less than 1200°C, this is supported by only 3 out of 12 data points in (24). The oxygen gradient in the stabilized alpha Zry layer dictates the speed of oxide/alpha interface movement during further oxidation at a different temperature. Parabolic kinetics will be reestablished as this oxygen gradient adjusts by diffusion to the new temperature. At temperatures above 1200°C, diffusion is so rapid that this adjustment occurs rapidly and little effect of preoxidation occurs. Such an effect cannot be modeled by parabolic rate laws, but rather by moving boundary diffusion models...It would therefore be concluded that the above results seem reasonable.

From Figure 5, it can be estimated that the average protective effects could be approximated to be about a 50% reduction in parabolic rate constants at about 1000°C, decreasing to zero at about 1200°C. If it is further assumed that this rate reduction is in addition to the scatter in the data, the protective effects of pre-films can be represented by the shaded area labeled "pre-film" in Figure 6. The magnitude of the prefilm effect in Figure 6 was found by multiplying the mean value by the enhancement factor, as will be done for all factors which affect oxidation rates. It can be seen from this figure that the scatter originating from prefilm effects is less important than the scatter in the isothermal oxidation data itself. Because the prefilm effects are reductions in rate constants, they are generally ignored in LOCA calculations, thus introducing an additional measure of conservatism (i.e., additional margin). In this context, the electrically heated experiments of Hagen et al. [38] have recently shown that oxide films formed during the earlier (heatup) stages of a LOCA delay the autocatalytic behavior of the Zircaloy-steam reaction and limit peak cladding temperatures to be less than 2200°C, about two-thirds of the original temperature predictions. Slower heatup rates permit thicker protective oxides which reduce both the reaction rate (longer diffusion lengths) and the total inventory of Zircaloy metal available for rapid exothermal reaction later in the LOCA.

Saturation of the Beta Phase

The interior beta phase approaches saturation with oxygen as the Zircaloy-steam reaction proceeds, whereas parabolic rate equations assume that there exists an infinite sink for the oxygen. Therefore, parabolic rate constants may appear to increase as the beta phase saturates. This is true for the oxide and alpha phase rate constants. However, the oxygen consumption rate constant decreases since the capacity of the Zircaloy to absorb oxygen is decreasing.

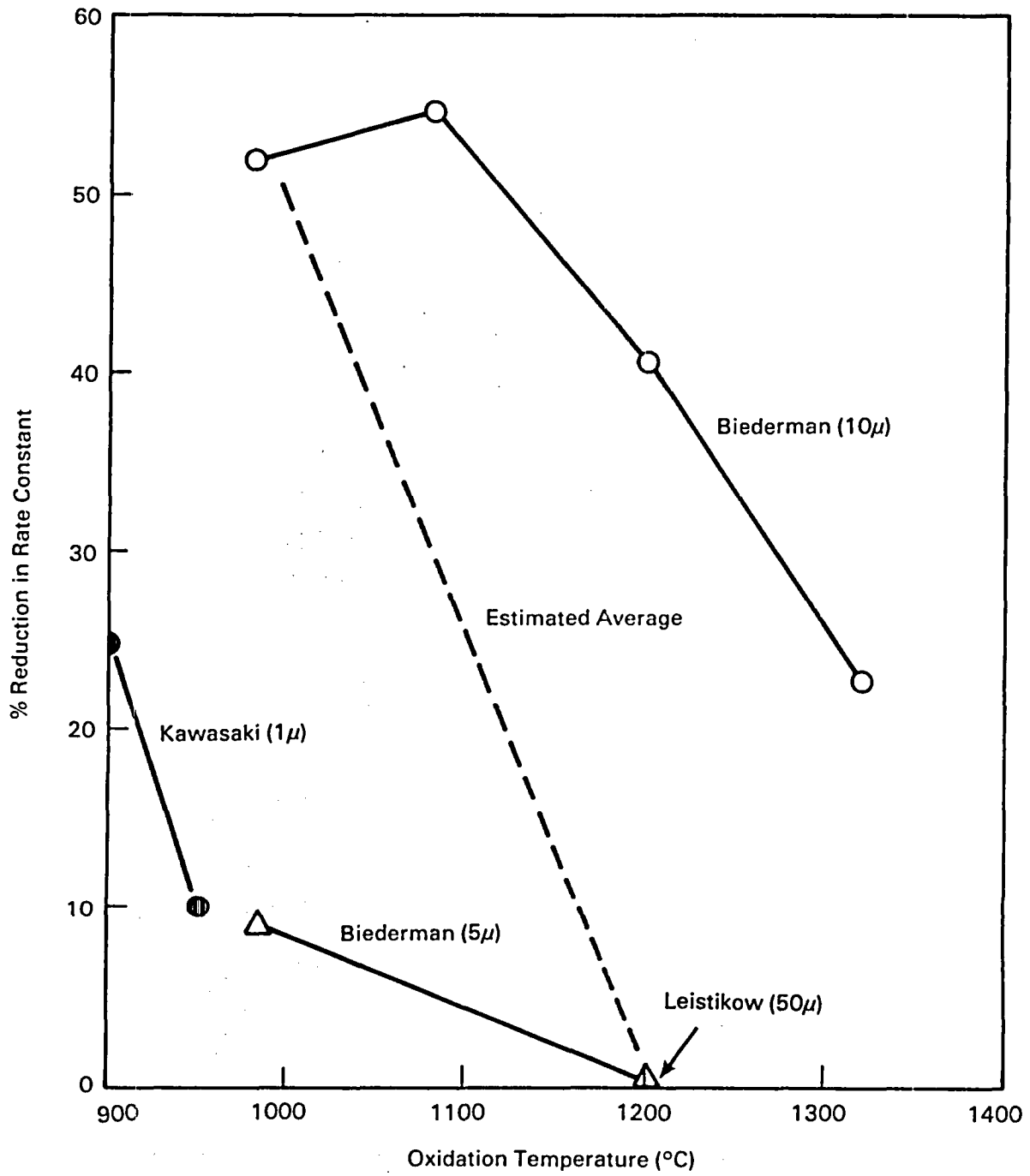


FIGURE 5. Reduction of Rate Constants by Pre-Films

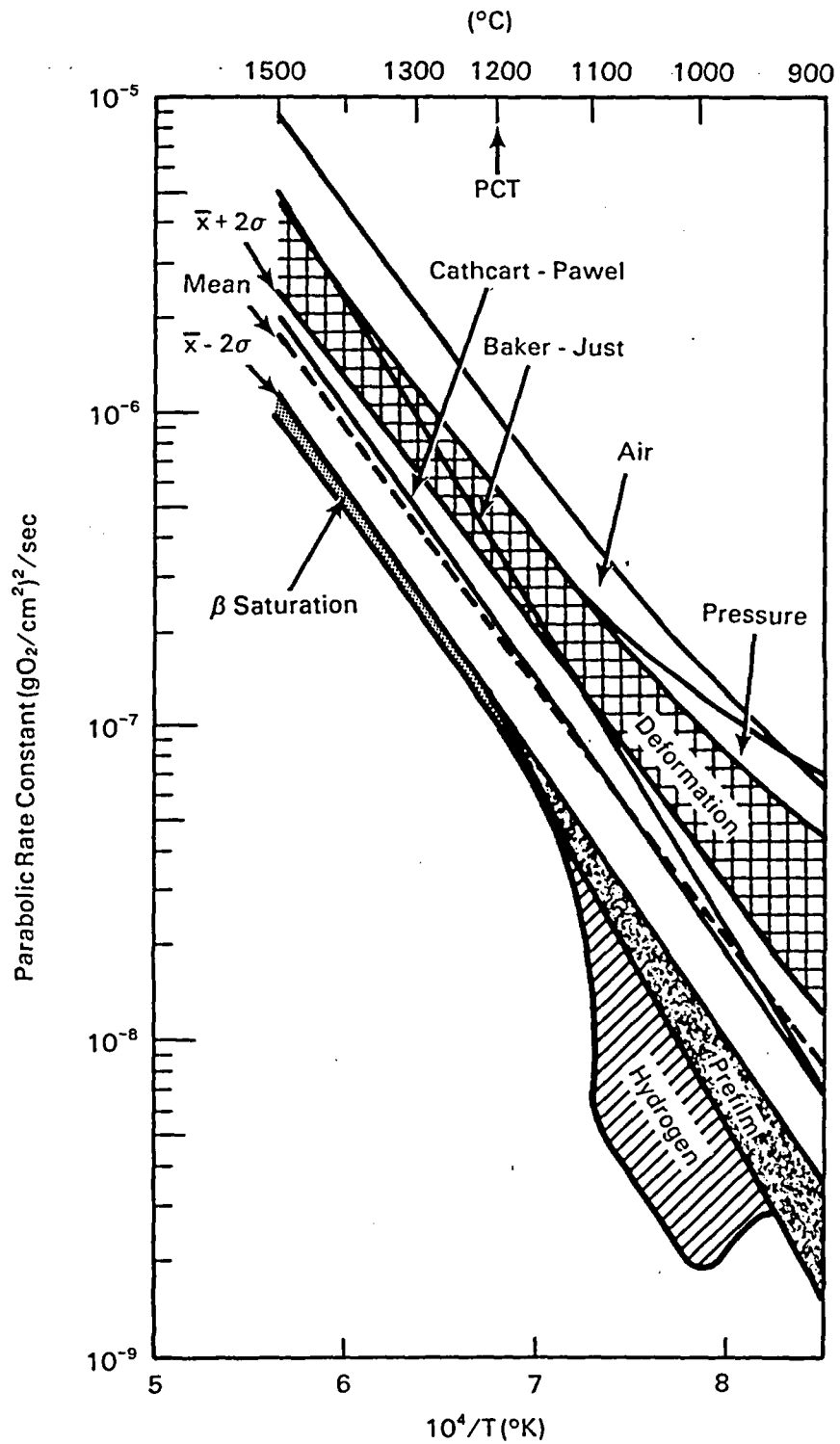


FIGURE 6. Factors Which Affect Oxidation Rate Constants (1000-1500°C)

Pawel and Campbell [39] have investigated this effect over the temperature range of 1000-1500°C. At 1300°C, they found that the initial parabolic rates were maintained for about 500 seconds for single sided oxidation. This is longer than the expected duration of a LBLOCA, as is even a very rough estimate for beta saturation during two-sided oxidation (250 seconds). However, the SBLOCA may have larger duration and these effects may be important. Pawel and Campbell report rate constant increases for non-deformed cladding of 3-17% and 45-135% respectively for the oxide and alpha phases, while the oxygen uptake rate constant decreases by 3-13%. The latter is shown in Figure 6, and is seen to be a minimal effect compared to the scatter in the data, adding a small conservatism to LOCA calculations.

In the higher temperature ranges (above 1500°C), Prater estimates that beta saturation introduces an uncertainty of +5% in oxide growth rates. Although this estimate has not been previously published in the open literature, it is shown in Figure 7. The oxide growth rate enhancement is assumed to be included in Prater's overall estimate of $\pm 35\%$ uncertainty, which is shown by the error bars in Figure 7. The oxide growth rate increase at high temperatures is seen from this figure to be a relatively small effect compared to the scatter in the data base itself. The effect is therefore generally ignored in numerical simulations of SFD scenarios which span this temperature range. It should be noted that Prater's disc samples are 0.9 mm thick, compared to typical PWR cladding wall thicknesses of about 0.69 mm. A thinner sample may thus make this effect relatively more important.

Deformation Enhancements

Depressurization of the primary coolant during a LBLOCA or SFD will permit cladding deformation (ballooning and possibly rupture) to occur because the fuel rod internal pressure may be greater than the external (coolant) pressure. In this case, oxidation and deformation can occur simultaneously. This in turn may result in an apparent enhancement of oxidation rates because (1) ballooning increases the surface area of the cladding and permits more oxide to form per unit volume of Zircaloy, and (2) the deformation may crack the oxide and provide increased accessibility of the oxygen to the metal. However, deformation generally occurs before oxidation rates become significant, i.e., below 1000°C. Consequently, the lesser importance of this phenomenon has resulted in a relatively sparse data base, as described below.

Knights and Perkins [40] reported oxidation rate enhancements of 1.2 to 2.0 for temperatures between 400 and 475°C and oxides thicker than about 2 microns when tensile stresses in the creep range were imposed on the sample. These enhancements occurred in steam and wet oxygen, but not in pure oxygen, and are shown in Figure 8. Bradhurst and Heuer [41] used the Zircaloy ring compression test in flowing steam at 700-1300°C to produce localized oxide thickness enhancements of up to about 2.15. Maximum enhancements occurred at slower strain rates, and a mechanism was proposed to explain this phenomenon. However, the overall weight gain or average oxide thickness in [41] was only minimally increased because of the localization effects of cracks in the oxide layer. Bradhurst's localized oxidation enhancements are shown in Figure 8.

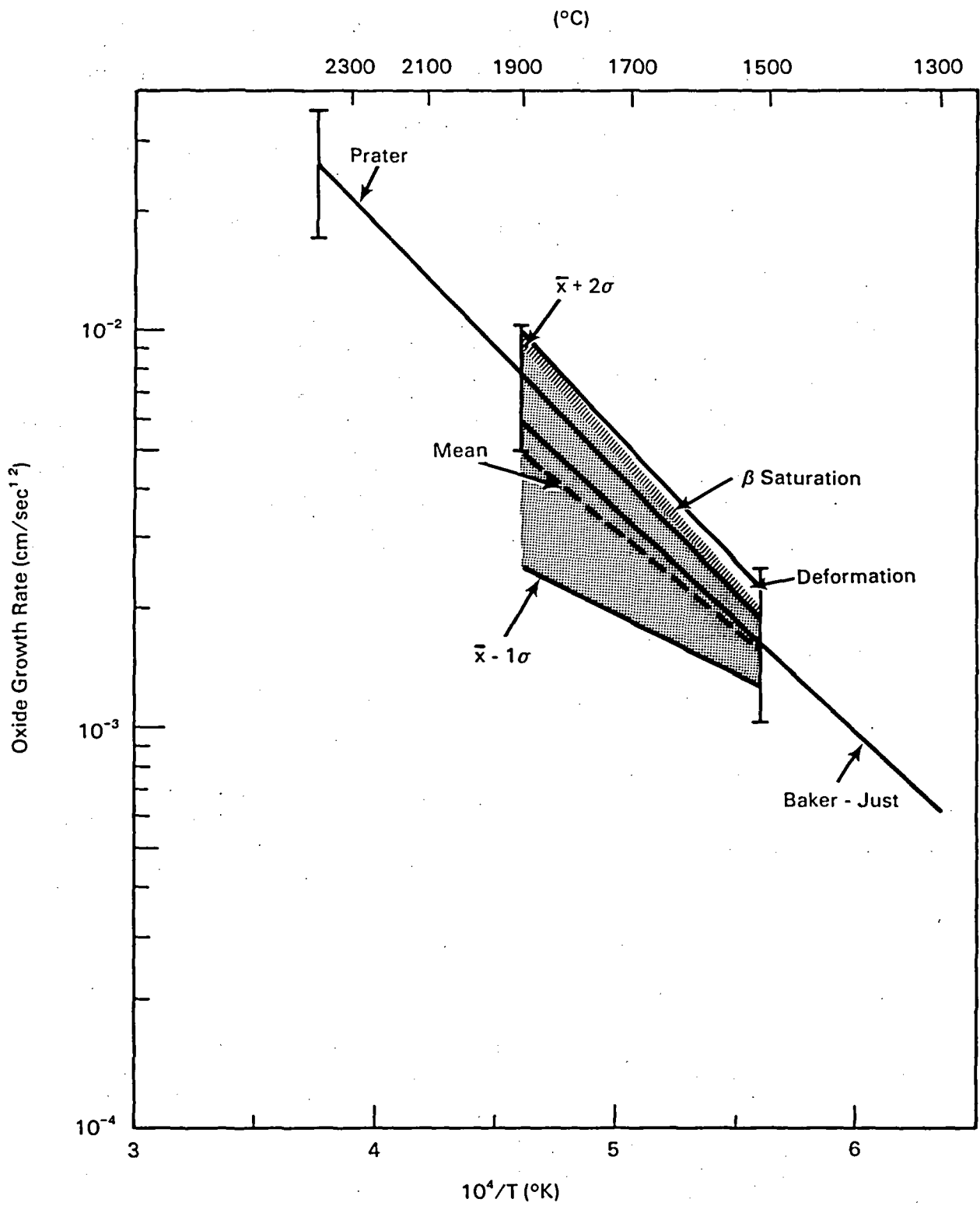


FIGURE 7. Factors Which Affect Oxidation Rate Constants (1500-2300°C)

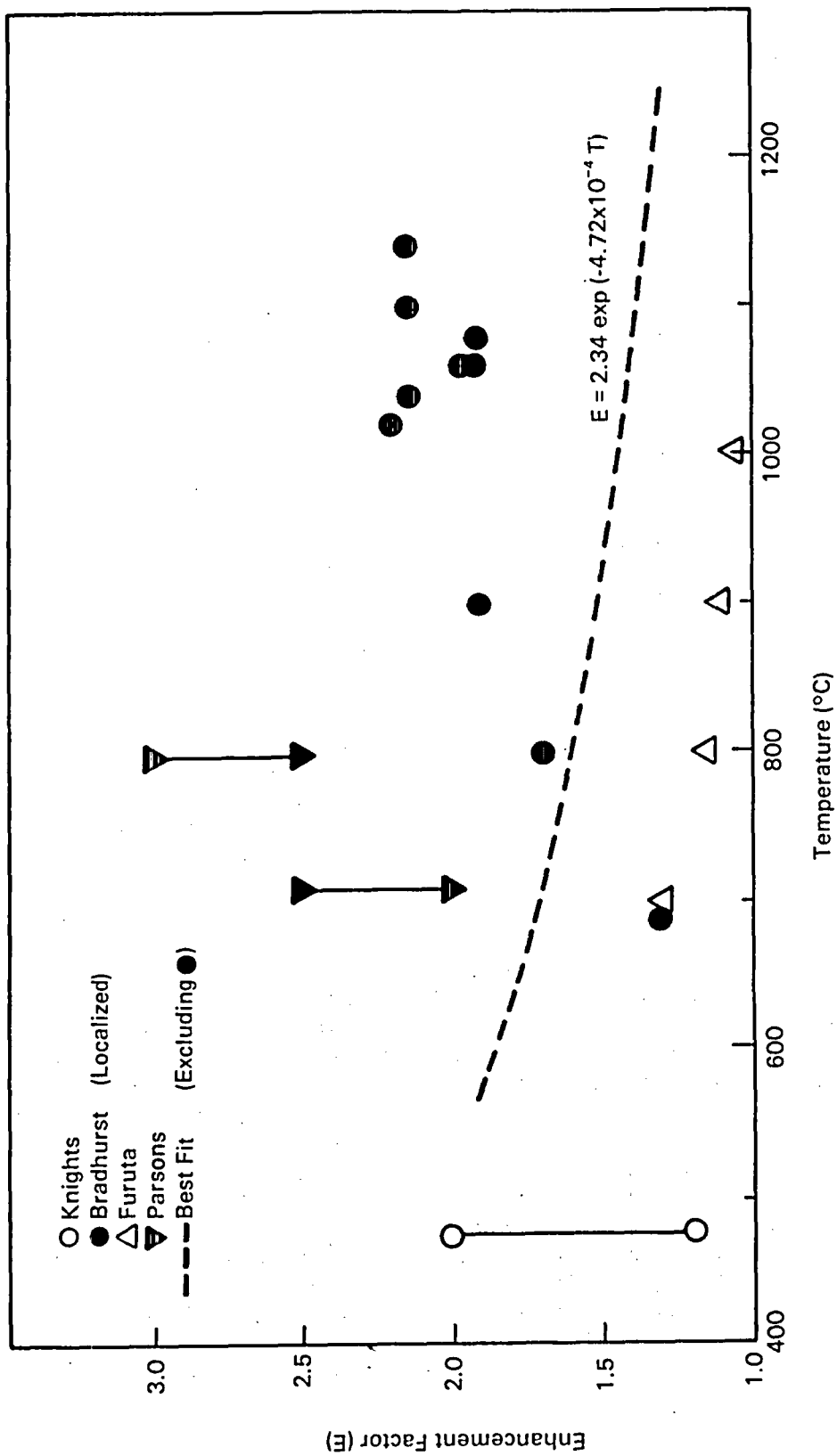


FIGURE 8. Oxidation Enhancement Factors Caused by Deformation

Leistikow and Kraft [42] used pressurized tubes to simulate simultaneous oxidation and creep at 900°C in either argon or steam for up to 30 mins. Increasing stress caused more oxide cracking and greater oxide thicknesses. However, the enhancement factor was not available at the time this report was prepared.

Furuta and Kawasaki [43] used tensile specimens axially strained to failure at a strain rate of about 2.8×10^{-2} /sec and simultaneously oxidized in steam at 700-1000°C to study deformation-induced enhancements. The results shown in Figure 8 decrease with increasing temperature and increase toward apparent saturation with increasing strain. The maximum oxide thickness enhancement of 1.3 occurred at 700°C and about 18% strain after about 300 sec of exposure to steam. Very small enhancements occurred at about 8% strain at 1000°C. The details of the oxide morphology were not reported.

Parsons and Hand oxidized pressurized Zircaloy tubing in flowing steam at 710 and 800°C. This work is described in [3]. Average diametral strains ranged between 5 and 30% after 5-7 hours of exposure, but localized strain ranged up to 80% at the rupture location. Weight gain enhancements of 2.0-2.5 at 710°C and 2.5-3.0 at 800°C were observed, being caused by the combined effects of increased surface area due to ballooning and by oxide cracking. Extensive oxide cracking was observed to occur at 10% strain at 710°C and at 5% strain at 800°C. Oxide thickness enhancements followed the same trend as weight gains, and are illustrated in Figure 8.

Although the data in Figure 8 are rather sparse, it is possible to make a very crude estimate of the expected average enhancement of oxidation kinetics by deformation. This is shown by the dashed curve in Figure 8, which was fit to the data points by least squares, and ignoring the localized enhancement data of [41]. The rate enhancement data of [40] were assumed to be of the form $\text{cm}/\text{sec}^{1/2}$. This average curve is taken to represent the oxygen uptake or oxide thickness enhancement, which is proportional to the square root of the enhancement in rate constants ($\delta^2/2$) because the deformed versus nondeformed samples were oxidized for the same time periods. The squares of the enhancement factors (E) are thus plotted in Figure 6, which shows that deformation induced enhancements introduce significant uncertainties in the parabolic rate constant for oxygen absorption over the lower temperature range. The effect is much less important in the higher temperature range, as shown in Figure 7, where the increased scatter due to E rather than E^2 is plotted. However, these effects are implicitly included in embrittlement/failure data, as will be seen in later discussions concerning the margins in the PCT and ECR criteria. Also, effects of increased surface areas on exothermic reaction heat generation and oxidation rates are accounted for in codes which simulate LOCAs. Therefore, deformation effects may not be a viable contributor to scatter in the parabolic rate parameters in Figures 6 and 7. The effects of internal stress distributions and metal strains caused by the volumetric expansions associated with oxygen uptake and oxide formation [reviewed in ref. 3] are also implicit in such data, but apparently do not affect the basic oxygen transport mechanisms [44].

Effects of Air

The reactor primary coolant system is pressurized during operation. The pipe break that occurs during a LOCA permits exit of this coolant. When the core becomes uncovered, steam is generated and also exits the break. The injection of ECCS fluid consumes the free volume in the core, forcing steam and/or fluid out of the break. At all times, the core pressure is expected to remain above the containment pressure at the pipe break, so that no air would be expected to enter the core. However, some experiments have been conducted to assess the effects of various gaseous impurities in the steam on oxidation rates. These data are included here for informational purposes.

The primary effect of air on Zircaloy-steam oxidation is an increase in the apparent oxidation rate. This occurs because the high nitrogen content of air (about 78% by volume) forms nitrides with the Zircaloy, which then oxidize and permit easier access of oxygen to the metal. The nitrides also have a higher Pilling-Bedworth ratio than the oxides, so the reaction film is prone to more cracking, which also may increase apparent oxidation rates. However, Cathcart et al. [45] added 10% nitrogen to steam at 1100 and 1300°C, and found no significant changes in oxidation rates. Leistikow et al. [46] oxidized Zircaloy tubes in steam and air for comparison of rupture test results, finding minimal effects on oxidation and rupture characteristics at temperatures below about 800°C. However, the effects of air were significant at 1000°C. Leistikow [28] also studied the effects of pure air, oxygen, and steam over the 900-1150°C temperature range. Interpretation of those plotted results shows an average weight gain enhancement factor of 1.4 at about 10 to 15 seconds of exposure time. Assuming the oxygen uptake to be proportional, this rate constant enhancement factor is the square of the above, or about two. The enhancement effects of air on this oxidation rate constant are shown in Figure 6. Note again that this is included for informational purposes only because air is not expected to enter the primary coolant system during a LOCA.

Effects of High Pressure Steam

Most Zircaloy oxidation experiments have been conducted at atmospheric pressure. However, the reactor core may remain significantly pressurized during a SBLOCA. The higher density of steam molecules at the oxide-steam interface has been postulated to enhance oxidation rates, although parabolic oxidation rate theories would predict no such effect of steam pressure. Pawel et al. [47] conducted experiments at 905 and 1101°C at steam pressures up to 10.34 MPa (1500 psi). No effect was found at the higher temperature. However, at 905°C either the monoclinic to cubic oxide phase transformation or oxide cracking [47] caused an apparent oxidation rate enhancement. From Tables 1 and 5 of [47], the estimated maximum enhancement factor for the oxygen uptake rate constant at about 410 sec and 10.34 MPa is approximately 2.9. This is shown in Figure 6, and is approximately the same enhancement factor as for air, but smaller than for deformation effects. It should also be noted that the null effect at 1101°C has been confirmed by Prater [33] who found no effect at higher temperatures, thus attributing the pressure enhancement to the oxide phase change.

Steam Starvation by Hydrogen Dilution

Steam dilution by the hydrogen generated from the Zircaloy-steam reaction has been postulated to slow the reaction rate in an effect called steam starvation. Such hydrogen may collect at the top of the core and result in insufficient oxygen availability for the reaction to proceed at normal rates, especially for SFD scenarios. Additionally, steam ingress into the narrow fuel-cladding gap after the cladding ruptures may be limited, so that local hydrogen overpressures may limit the reaction rate at the cladding inner surface. These effects were investigated because a reduction in reaction rates would naturally render a LOCA less severe in terms of Zircaloy oxidation. The research performed is outlined below.

Westerman [48] noted hydrogen-induced reductions in oxidation rates as early as 1962. Furuta et al. [49,50], Kawasaki et al. [51], Uetsuka [52], Furuta [53], and Chung/Kassner [5] observed different oxide morphologies on the inner and outer surfaces of simulated fuel rods ruptured and oxidized in flowing steam. The influence of such inner oxides on hydrogen uptake by the Zircaloy is implicit in much of the laboratory data concerning embrittlement. Homma et al. [54] and Furuta et al. [55] tested the oxidizing effects of flowing hydrogen/steam mixtures on non-deformed cladding over the temperature range 950-1100°C. The hydrogen/steam ratio ranged between 0.05 to 2.0 by volume and steam flow rates ranged between 0.5 and 18.3 cm³/sec. They found that hydrogen/steam ratios above about 30-40% produced significant reductions in total weight gains at the lowest flow rate and for temperatures above about 950°C. A graphical interpretation of the data from Figure 3 of [55] is shown in Figure 9. The effect of the high hydrogen concentration on the oxygen uptake rate constant is estimated in Figure 6. This effect has been associated with the monoclinic to tetragonal phase transformation of the oxide, and vanishes as temperatures approach about 1200°C. The latter conclusion is supported by recent data from Uetsuka [56] and Prater [33], who found no effect at temperatures of 1300°C and 1565 to 1800°C, respectively, for molar hydrogen dilutions of up to 90%. Earlier data by Chung and Thomas [30,57,58] indicated that the Zircaloy-steam reaction could be significantly retarded at hydrogen concentrations of 50% to 70%. However, Prater's studies [33] suggest that these results may have been affected by steam starvation inadvertently introduced in the experiment by low steam flow rates. Also note that the flow rates associated with the data depicted in Figure 9 may be lower than expected in a LOCA.

Although it may be possible for low steam flow rates and for high hydrogen concentrations to occur during an SFD scenario, a recent consensus reached the conclusion that hydrogen-induced steam starved conditions should not be assumed for ECCS calculations. This result is partly due to data from Uetsuka [56] who found that the Zircaloy-steam reaction was about 85% efficient at 1300°C. That is, 85% of available steam was reacted whenever it was present. Although the above consensus assumption to not permit hydrogen-induced steam starvation seems reasonable for the cladding outer surface, the oxide morphologies observed on the inner surfaces of ruptured rods may indeed affect hydrogen uptake by the Zircaloy, and thus the embrittlement effects.

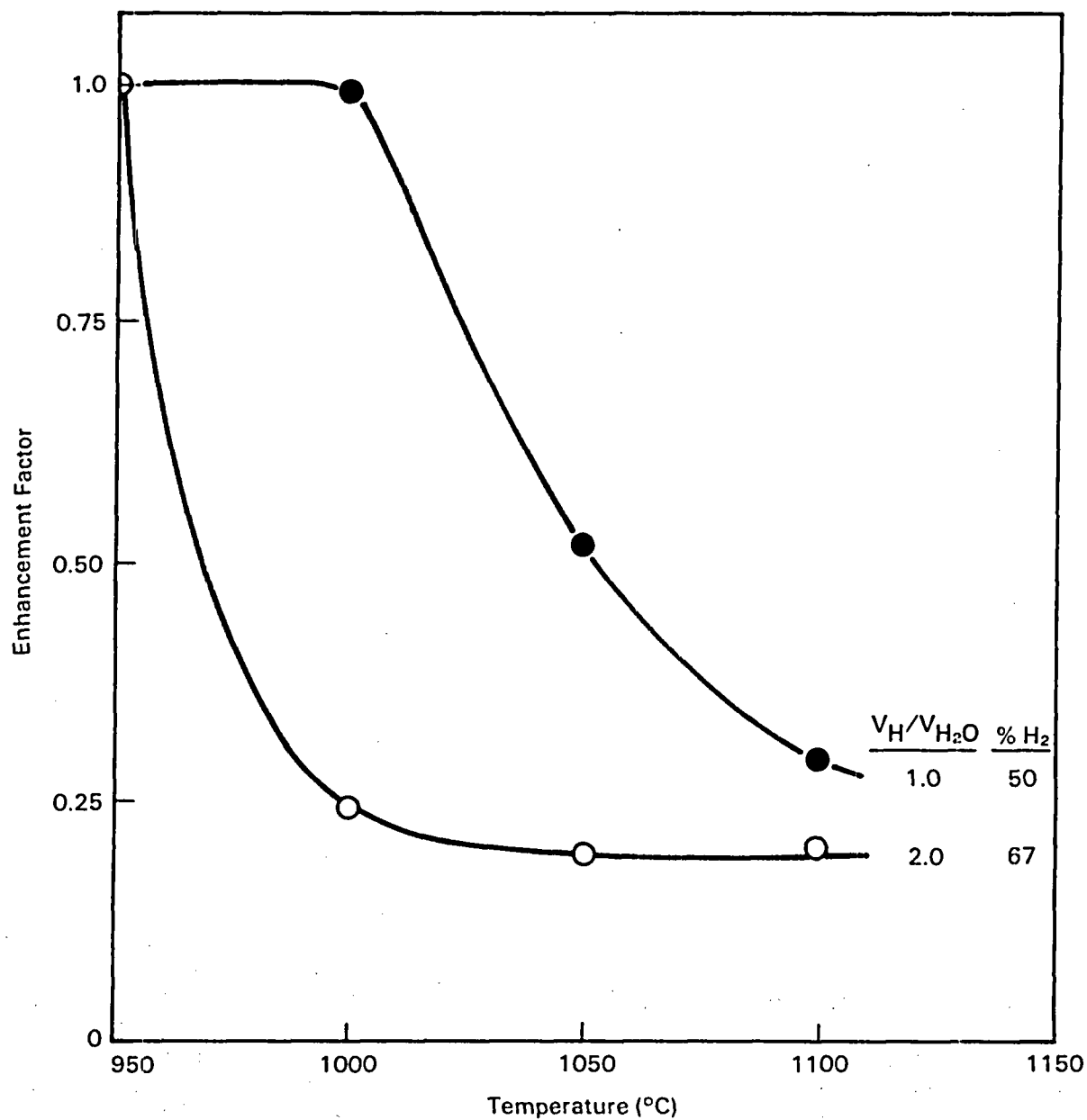


FIGURE 9. Enhancement Factor for Hydrogen Dilution

4.1.3 Margins in the Oxidation Rate Data

The term "margin" as used in this report refers to the difference between the prediction by a current method (i.e., criterion) and the expected extreme value as evaluated from the data base. In this case, extreme value is taken to be the maximum expected oxidation rate, which results in the minimum time to reach 17% ECR at the 95% confidence level. The percent margin is simply the above difference divided by this expected extreme value. The margin is thus the amount of conservatism over and above the expected extreme value, which is defined as the mean plus two standard deviations ($\bar{x}+2\sigma$ in Figures 3 and 4) plus other factors which may increase this maximum value (Figures 6 and 7). These other factors for the two temperature ranges above and below 1500°C are discussed below.

For the low temperature regime ($T < 1500^\circ\text{C}$), the effects of steam pressure are included in the expected maximum value for the parabolic oxygen uptake rate constant. Deformation effects are excluded because they are accommodated in other submodels of LOCA simulation codes by virtue of the oxygen uptake rate being a function of the surface area of the cladding. Deformation effects are also excluded for the high temperature (above 1500°C) regime, but the effect of oxygen saturation of the beta phase is included because oxidation rates are so rapid that saturation may be approached quickly. Beta saturation amounts to about a 5% increase in oxide growth rates, as estimated by Prater [33].

The basis for the margin assessment at low temperatures is shown in Figure 10, where the margin is shown by the shaded region. The resulting percent margins in Figure 11 indicate that a negative margin exists below about 1100°C with respect to the maximum expected oxidation rates. However, there is a growing consensus that the mean value of the parabolic rate constants should be used in this temperature regime. It is believed that knowledge of Zircaloy-steam oxidation behavior has been sufficiently improved by the research of the last decade to allow this to be done with confidence. The Cathcart-Pawel rate constant is frequently considered to be a sufficient approximation of the mean to permit its use as a new element of the ECCS Acceptance Criteria, replacing the Baker-Just correlation. The end result of this action would be to remove all margins from oxidation calculations, yielding best-estimate rather than conservative predictions. This seems reasonable in comparison to the inconsistencies in the Baker-Just relation and its associated margin. Removal of margins in this portion of the ECCS Acceptance Criteria will place greater importance on margins concerning cladding embrittlement and failure by thermal shock, i.e., the 1204°C and 17% ECR limits. Margins in these criteria will be discussed in a later section of this report.

The current margins for the oxide growth rate constant in the high temperature regime are shown in Figures 7 and 12. Figure 7 shows a scatter comparable to that indicated by Baker [59] in a recent paper. The current criterion (Baker-Just) yields a negative margin with respect to the expected maximum in the data base. Replacements for the Baker-Just correlation are also being considered for temperatures above 1500°C. However, in this case the data base is still rather sparse, and the mean is not as well defined as for lower temperatures. The Prater-Courtright [33] oxide growth rate correlation has

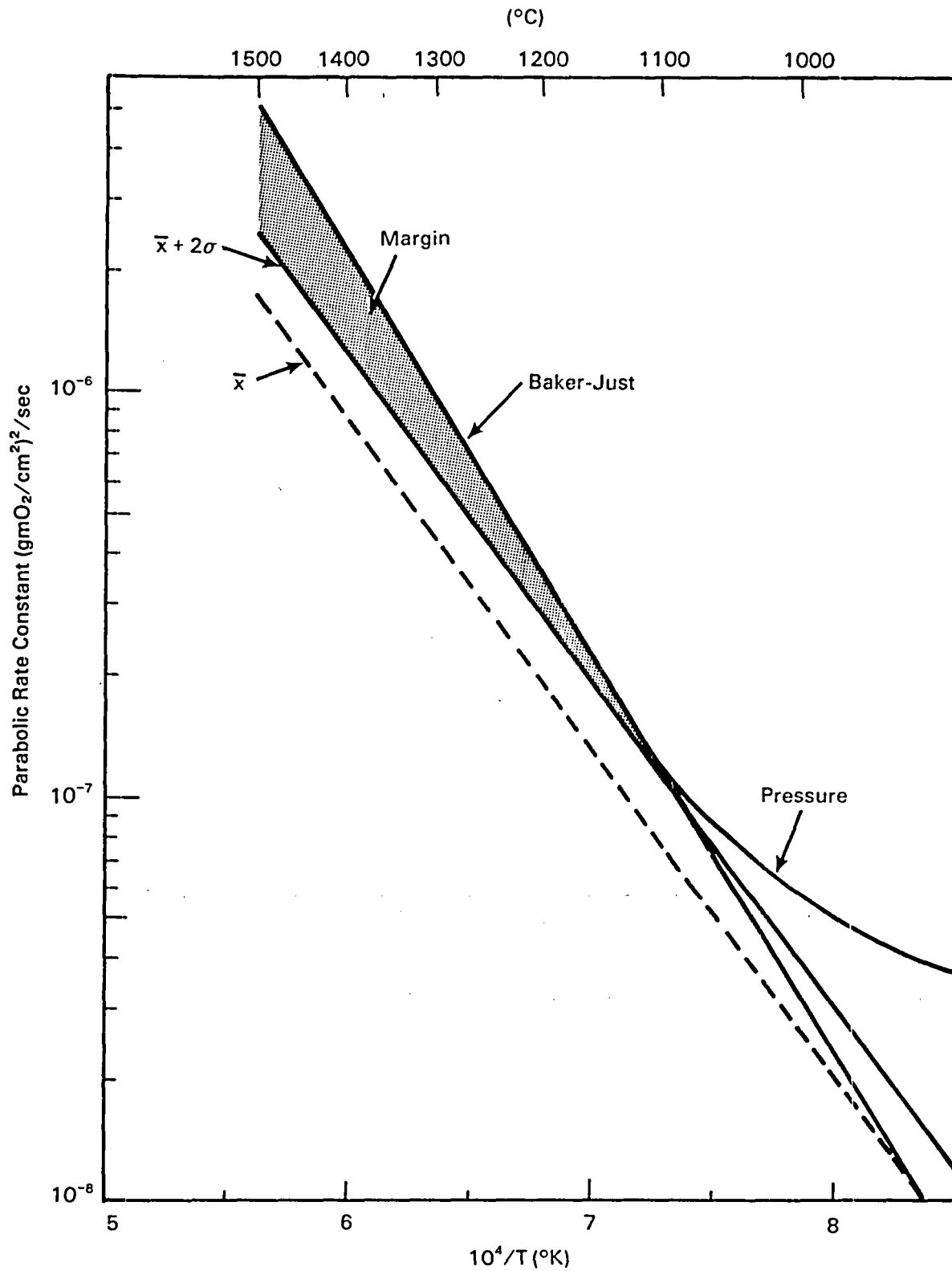


FIGURE 10. Basis for Oxidation Rate Constant Margin Assessment at Lower Temperatures

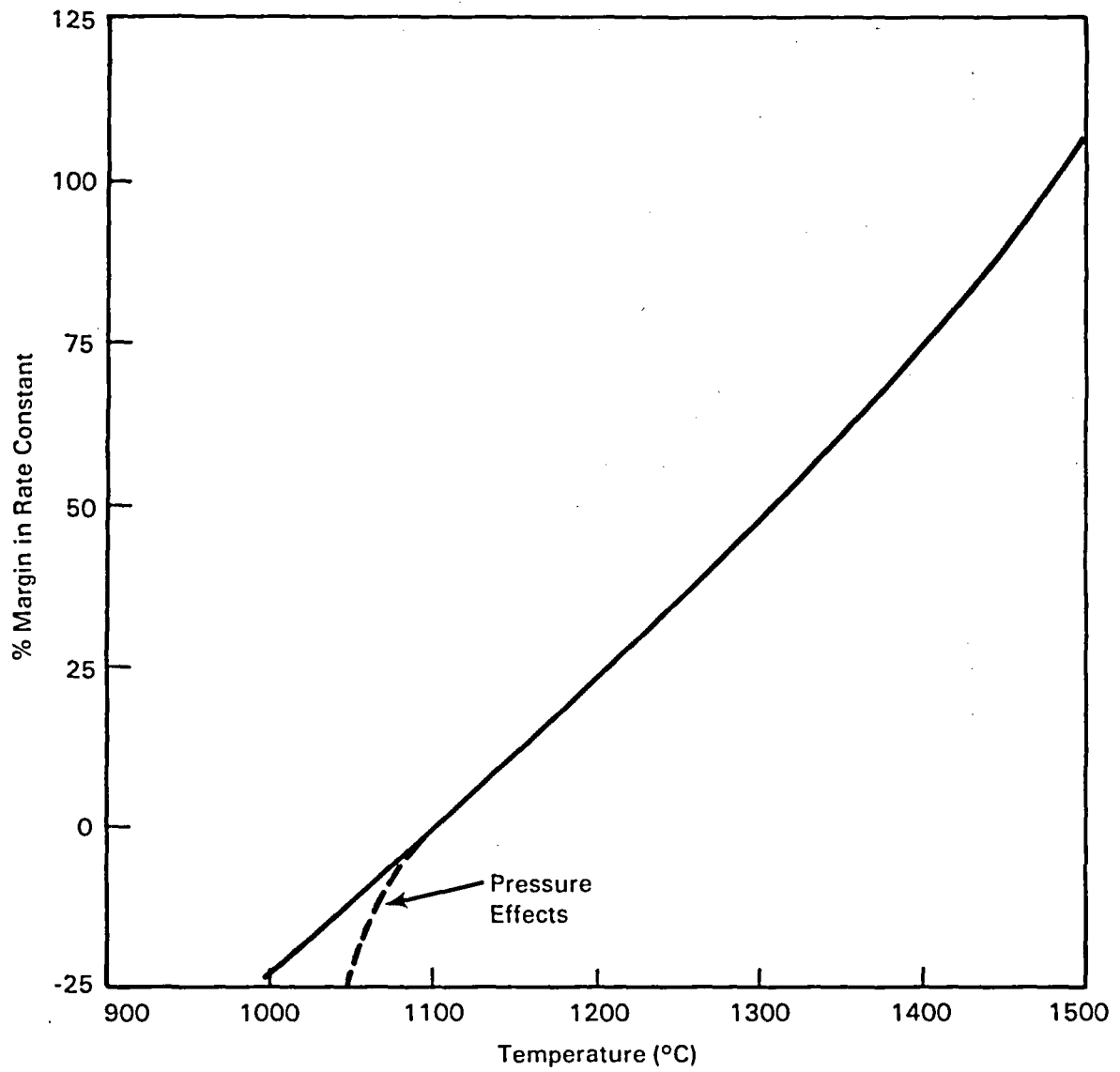


FIGURE 11. Percent Margin in Oxidation Rate Constants at Lower Temperatures

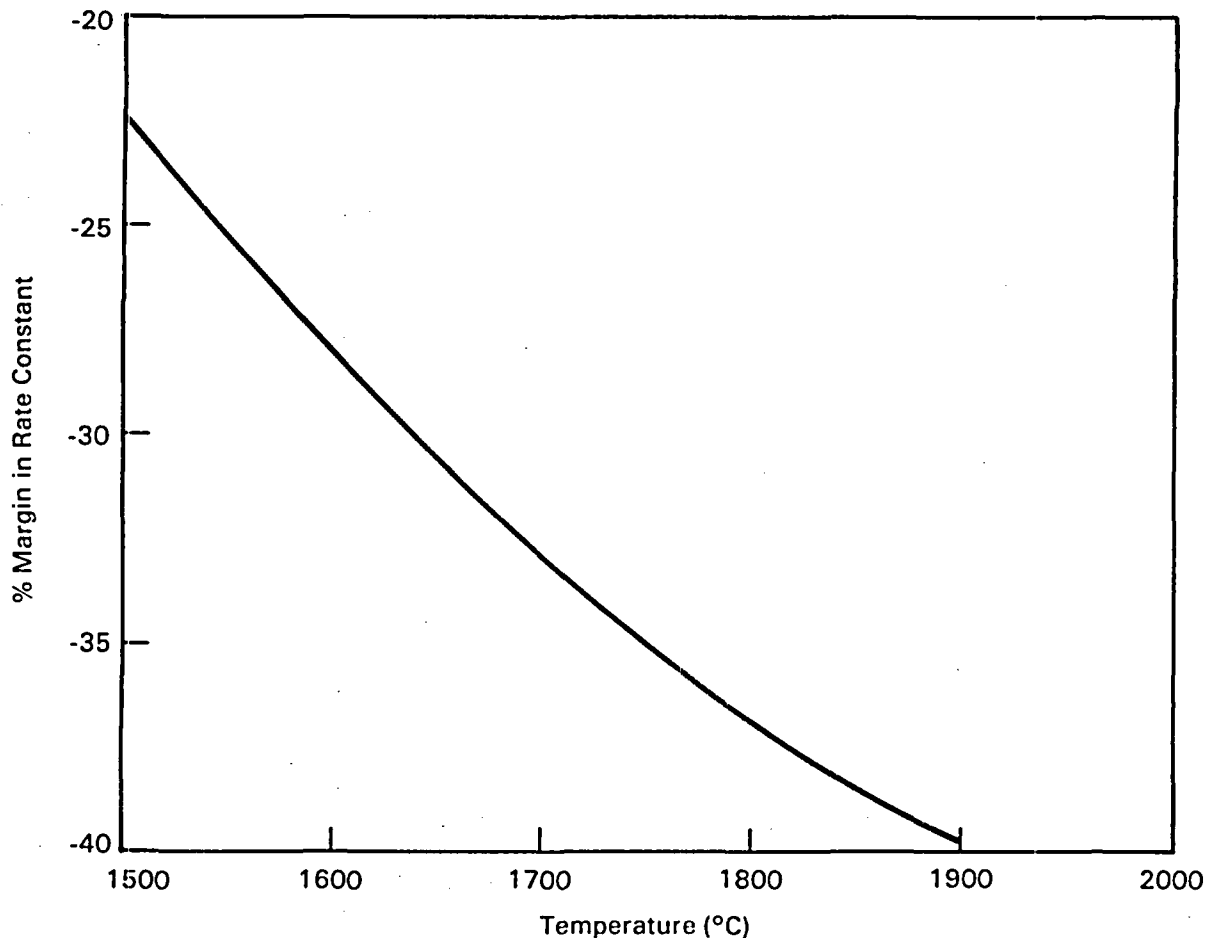


FIGURE 12. Percent Margin in the Oxidation Rate Constants at Higher Temperatures

been proposed to replace the current Baker-Just requirement in the criteria. The Prater-Courtright relation corresponds to the mean plus about 1.3 standard deviations of the current data base for temperatures of 1500-1900°C. This is a reasonable safety margin above the mean, but does not bound the expected maximum value of the current data base. If such an upper bound is desired, Prater's uncertainty of 35% [33] clearly performs this function and can be added to his correlation for calculations of Zry-steam oxidation behavior during a LOCA or SFD scenario.

4.2 EMBRITTLMENT OF ZIRCALLOY DURING OXIDATIONS

The main purpose of the ECCS Acceptance Criteria is to ensure that a coolable core geometry is maintained during and after a LOCA. The loss of coolable core geometry may occur when the Zircaloy cladding becomes sufficiently embrittled by steam oxidation so that the cladding would shatter upon cooldown or

during post-LOCA removal of the fuel rods from the reactor core. Such fractures may permit fuel and cladding fragments to fall to the bottom of the core, creating a rubble pile. The cooling characteristics of such a rubble pile were not known at the time of the ECCS hearings, and the criteria thus apply both to thermal shock during the LOCA and to handling forces during rod removal after the LOCA. It is the purpose of this section to assess the safety margins in the two quantitative embrittlement criteria for both cases. The specific criteria to be addressed are the 1204°C PCT and the 17% ECR limits. The PCT limit prevents the cladding from entering a temperature regime where the oxidation reaction accelerates and embrittlement occurs rather quickly, while the ECR limit specifies the maximum amount of oxidation allowable at temperatures below the PCT. The other criteria pertaining to embrittlement are qualitative in nature, and specific margin assessments are not possible with the methods used in this report.

4.2.1 Recent Research Results

Zircaloy oxidation-embrittlement research performed in the last decade include both in-reactor and laboratory experiments under various conditions. Although the data from each source are frequently voluminous, the number of independent investigations is substantially less than for the reaction rate data addressed in Section 4.1 of this report. Because in-reactor oxidation and embrittlement is a rather complex process, the following paragraphs will concentrate on experiments which have attempted to emulate fuel rod behavior by employing either actual or simulated fuel rods. Such experiments implicitly include effects such as cladding deformation/rupture and hydrogen absorption. However, the axial restraint provided by the grid spacers in power reactors has usually been neglected, even though these forces may be quite important in determining the fracture behavior of the cladding during the thermal shock which occurs during quench. Some data are available to assess the effect of axial forces on the PCT and ECR margins and are also reviewed below.

Thermal Shock Data

Chung and Kassner [5] developed an extensive oxidation embrittlement data base for Zircaloy cladding for both thermal shock and impact/handling over temperatures ranging from about 800°C to about 1500°C. The thermal shock experiments employed standard Zircaloy-4 cladding with 0.635 mm wall thickness. The 200 mm long simulated fuel rods were filled with alumina pellets sized to produce a 0.20 mm diametral fuel-cladding gap and prepressurized with helium or argon at 6.89 MPa. The cladding was heated directly with an ac power supply at about 10°C/sec up to the isothermal oxidation temperature, which was maintained to within ±7°C in a flowing steam atmosphere at 0.06-0.08 MPa. Temperatures were measured by 5 thermocouples attached to the cladding outer surface. Cladding specimens typically ruptured at about 750°C, exposing the inner surface to the steam atmosphere. Although the effects of hydrogen absorption and two-sided oxidation of the cladding are implicit in these experiments, this is probably not the case for axial restraint. The tube ends were secured by standard pressure tubing fasteners, which can slip under axial loads. There is also no mention in [5] that the fasteners may have been axially restrained.

After a specified time period at temperature for oxidation, the simulated fuel rods were cooled by either of two methods to study the effect of cooling rate on the microstructure of the prior beta region (see Section 2). Fast cooling at about 100°C/sec was achieved by bottom-flooding the experimental apparatus with water within about 3 seconds, producing violent boiling. Nucleate boiling was established at the Liedenfrost point at about 500-570°C. Slow cooling through the alpha plus beta range of the Zircaloy was controlled at about 5°C/sec, followed by bottom flooding with water at about 827°C. The cooling rate in the final cooling stage was about 970°C/sec, producing about the same thermal shock for the two cooling methods [5]. The data produced by this experimental method are shown in Figure 13, where the effect of a fast cooling rate is seen to reduce the allowable time at temperature by about a factor of two [5]. The curves in Figure 13 were "best fit" in [5] and interpreted graphically from [5] and [60]. It is also of note that Chung and Kassner observed an effect due to the heating method: at temperatures below about 1277°C, cladding temperatures in ballooned regions were less than in non-ballooned regions because of a fin-cooling effect. Axial temperature gradients as large as 160-180°C were observed. Consequently, fractures occurred in non-ballooned regions for maximum temperatures below about 1250°C, and in ballooned regions for maximum temperatures above about 1327°C, the latter dominated by the effects of cladding wall thinning that occurs during ballooning and rupture. Other handling failure experiments also performed by Chung and Kassner [5] will be described below.

Furuta, et al. [61] also used Zircaloy-4 tubing with alumina pellets to simulate thermal shock behavior. The cladding had a wall thickness of 0.725 mm, the fuel-cladding diametral gap was 0.30 mm, and the simulated fuel rods were 500 mm long. The rods were heated in an infrared vertical tube furnace in flowing steam at 267 g/m² sec and temperatures were monitored by three thermocouples attached to the cladding outer surface. After the pre-pressurized rod simulators ruptured and were oxidized at predetermined isothermal temperatures (900-1300°C) for the specified amounts of time, cooling was achieved by bottom flooding with water at the oxidation temperature (fast cooling at about 300°C/sec) or by cooling slowly (5°C/sec) to 500°C and then bottom flooding. Some of the experiments were equipped with an electronically controlled load cell that provided axial restraint at the end of the isothermal oxidation period. The data are shown in Figure 13. Although the curves are not fit by any statistical means, the non-restrained cases appear to match the data of [5] rather closely above about 1150°C. At lower temperatures, in the monoclinic-tetragonal phase transformation region for the zirconia, the failure times are increasingly less than in [5]. Axial restraint reduces the allowable oxidation time by a factor of about two, similar to the effects of cooling rate in [5]. All axially restrained rods which failed did so at axial loads less than 1.5 KN, and cooling rate had no discernable effect for the restrained rods. Failures occurred randomly along the axis of the rod simulator in these experiments, and no correlation between oxidation and failure position could be found. Significant amounts of hydrogen upake also occurred at the cladding inner surface.

A series of 56 fuel rods were tested in the Power Burst Facility (PBF) in Idaho under the Irradiation Effects and Power Cooling Mismatch Programs. The

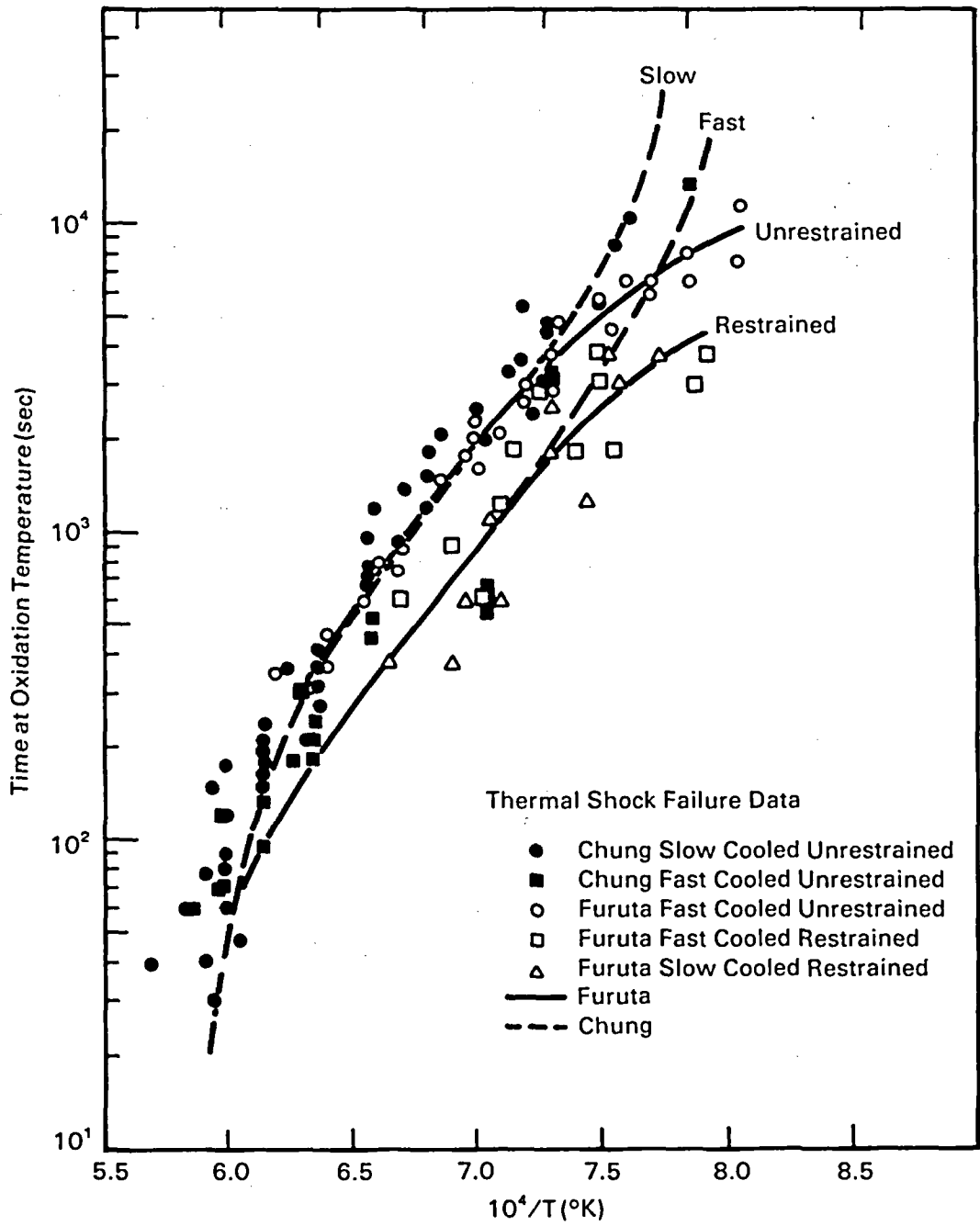


FIGURE 13. Thermal Shock Failure Data: Laboratory Experiments

data and their relation to the ECCS Acceptance Criteria have been discussed by Haggag [62]. A total of 16 separate in-reactor experiments were conducted in a pressurized water loop in the PBF. The fuel rods were 914 mm long, with cladding wall thickness ranging from 0.59 to 0.62 mm. Cladding temperatures were measured by three thermocouples attached to the outer surface. The general PBF test sequence consisted of thermal-hydraulic power calibration, a preconditioning period to crack and/or restructure the fuel, and testing under film boiling conditions. Film boiling was achieved by either decreasing the coolant flow rate or increasing power at low coolant flows. Heating rates were about 50°C/sec, and cooling rates were about 100°C/sec from test temperatures down to about 327°C. Of the 56 rods tested, 16 were preirradiated at burnups up to 16 GWd/tU. No effect of pre-irradiation was found for either thermal shock or handling failures [62]. There were 13 thermal shock failures and 9 handling failures. The thermal shock failures shown in Figure 14 all occurred for oxidation temperatures above the 1204°C PCT, as did the handling failures. The PBF experiments apparently contained no provision for axial restraint because instrumentation included rod elongation sensors.

Other data for the assessment of thermal shock failures are very scarce, and apparently consist of a single rod failure experiment at CRNL, briefly described in [60] and shown in Figure 14. However, some noteworthy experiments have been conducted in the NSRR facility in Japan [63-66]. More than 400 tests were conducted to study cladding oxidation and fuel rod behavior under reactivity initiated accident (RIA) scenarios. The fuel rod designs were very similar to those used in U.S. research programs. The tests were generally run with low fuel rod internal and coolant pressures so that the conditions may be similar to some depressurized LBLOCA scenarios. Cladding temperatures were measured by thermocouples attached to the outer surface. The results of these experiments showed that the cladding could survive measured temperatures as high as 1727°C for two or three seconds without loss of rod-like geometry during quench. These data are not shown in Figure 14 because the rods did not fail.

Handling Failure Data

The ECCS Acceptance Criteria were established partly based on the data from ring compression tests [9]. However, Furuta, et al. [61] noted significant differences in the compression to failure results for short ring specimens as opposed to longer sections of oxidized Zircaloy tubing. These differences were attributed partly to the effects of hydrogen uptake at the inner surface of the burst cladding. The relatively few ring-compression data sets generated in the last decade [5,61] also show considerable discrepancy, presumably caused by differences in experimental methods [3]. The characterization of handling failure propensity by such an ill-conditioned data set seems questionable, especially in view of the fact that the diametral compression loads during rod removal, transport, and storage operations are essentially unknown in terms of magnitude and mode of application. The ring compression test appears to be a specialized experimental method devised for a specialized application. However, impact testing has a much longer historical background with substantially better technical foundations. Further, impact conditions may provide better analogies to the more severe loads anticipated during rod

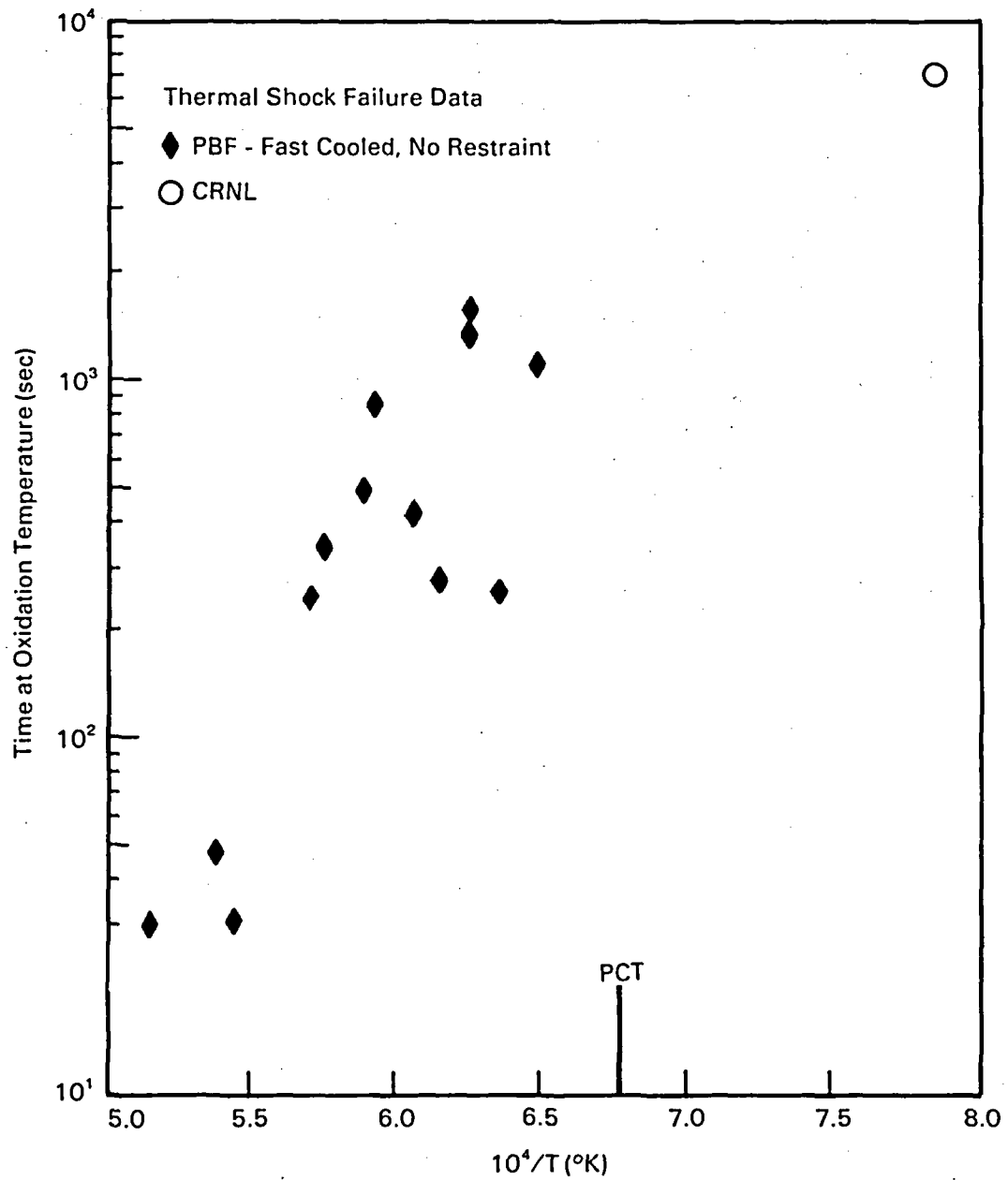


FIGURE 14. Thermal Shock Failure Data: In-Reactor Experiments

removal by overhead crane, accidental rod drop during removal or storage operations, or transport conditions. Consequently, this report will address handling failures in terms of laboratory impact and in-reactor rod removal data only, which provides an apparently more consistent data base to assess margins.

An extensive impact failure data base was developed by Chung and Kassner [5] using the same Zircaloy cladding as in their thermal shock experiments. Both undeformed and deformed cladding specimens subjected to the fast and slow cooling schedules previously described were impact tested at room temperature after oxidation. The 152 mm long undeformed samples were oxidized on both inner and outer surfaces by flowing steam, and then impact tested in-situ by a pendulum apparatus. The deformed cladding specimens were those that survived the slow-cooled thermal shock experiments previously described, and were tested on the same pendulum apparatus. The data are shown in Figure 15, where no significant difference between the various types of ANL data can be seen. All laboratory data shown in this figure failed at impact energies less than or equal to 0.3 J.

In-reactor data related to handling failures are apparently limited to the PBF data, which were described above and are also shown in Figure 15.

4.2.2 Margins in the PCT Criterion

Margins in the PCT limit will be assessed in a manner similar to the assessment of margins in the oxidation rate correlations described in earlier sections of this report. Margin is here defined as the difference between the lowest expected bound of the data and the value of the criterion. The general approach for computing the lowest bounds for thermal shock and handling failures is as follows. A best estimate curve fit to a particular data set is first determined by linear regression. The best estimate (or mean) curve is then corrected for biases originating from such sources as cooling rate or axial restraint effects. Then the 95% confidence interval is subtracted from the corrected best estimate to produce an estimate of the lowest expected bound for in-reactor conditions. Subtracting the value of the criterion (i.e., 1204°C) from this lowest expected bound then produces the minimum margin expected for in-reactor conditions.

PCT Margin for Thermal Shock

Two data sets are of possible use to determine the PCT margin for thermal shock: the in-reactor PBF data [62] and the ANL laboratory experiments [5]. However, these data apparently cannot be combined to form a single data set because of the bias which can be seen by comparing Figures 13 and 14. The PBF oxidation times to failure are obviously longer than the ANL times for the same temperature, even though the average wall thickness of the PBF cladding was slightly less. This effect may have been caused by the relation between wall thickness and the hoop stress caused by thermal shock. Although about two-thirds of the ANL data is at temperatures above the PCT limit, the PBF data set was selected to determine the PCT margin for thermal shock because the data originated from actual in-reactor experiments.

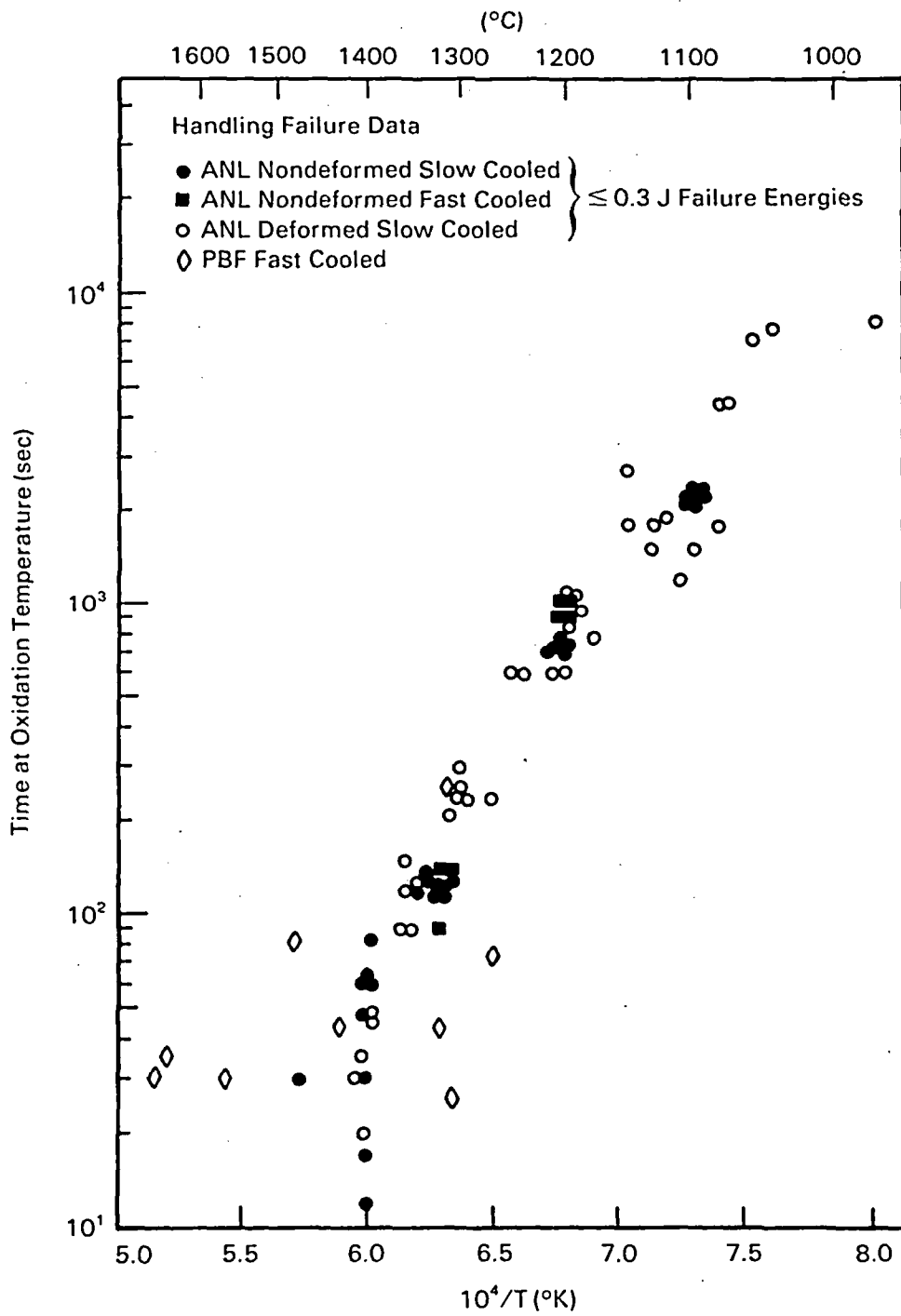


FIGURE 15. Handling Failure Data

The PBF data for fast-cooled thermal shock failures are repeated in Figure 16, along with a curve best fit by the least squares method. The correlation coefficient for this curve is a relatively low $r^2 = 0.73$. Because the PBF data were classified as fast-cooled, no correction is required. However, there was no axial restraint in these experiments because the rods were too short to require grid spacers as in power reactors. Therefore, the best estimate failure times are reduced by the factor of two determined above by comparison of restrained versus non-restrained thermal shock failures in the laboratory.

The confidence interval for in-reactor thermal shock failures was estimated using standard statistical techniques [67]. The value of the product $tV^{1/2}$ represents two standard deviations about the mean, or a 95% confidence interval. t is the value of Student's t for 95% confidence and for the given number of data points (n), and V is described by

$$V = \sigma^2 \left[1 + \frac{1}{n} + \frac{(X-\bar{X})^2}{\sum_1^n (X_i - \bar{X})^2} \right] \quad (5)$$

with

$$\sigma^2 = \frac{1}{n-2} \sum_1^n (y_i - \hat{y}_i)^2 \quad (6)$$

and \hat{y}_i is the expected value of the curve fit at X_i

\bar{X} is the mean of all X_i

X is the value of the independent variable at which $tV^{1/2}$ is evaluated.

For the curve fits in this report, the independent variable was chosen as $X = 10^4/T(^{\circ}\text{K})$ or as the natural logarithm of $10^4/T$, depending on whether the curve fit was linear or logarithmic. Logarithmic curve fits were frequently used in an attempt to reproduce the downward trend in the time-temperature curves at high temperatures commonly found in the literature [5,60], and shown in Figure 13. The dependent variable y was chosen as the common logarithm of the failure time in seconds.

Note that the above formula for V contains the number 1 enclosed within the parentheses. This means that the lower bound to be computed provides a 95% confident estimate that the next data point to be collected will fall within the confidence interval for the failure time. It is assumed here that the next data point will originate from a LOCA in a commercial reactor. Deleting the 1 in the parentheses of the V equation provides the 95% confidence interval for the best fit correlation itself, and is not of immediate use in the present analysis. Also note that the V formula is valid only for the next single data point, but not for all future data. Estimation of confidence intervals for the latter requires much more sophisticated statistical techniques [68]. The confidence interval was estimated using the expected values (\hat{y}_i) from the original best fit correlation, not the curve corrected for restraint effects. However, the computed confidence interval was subtracted from the corrected mean (labeled "Restraint Effects" in Figure 16) to produce the lowest expected

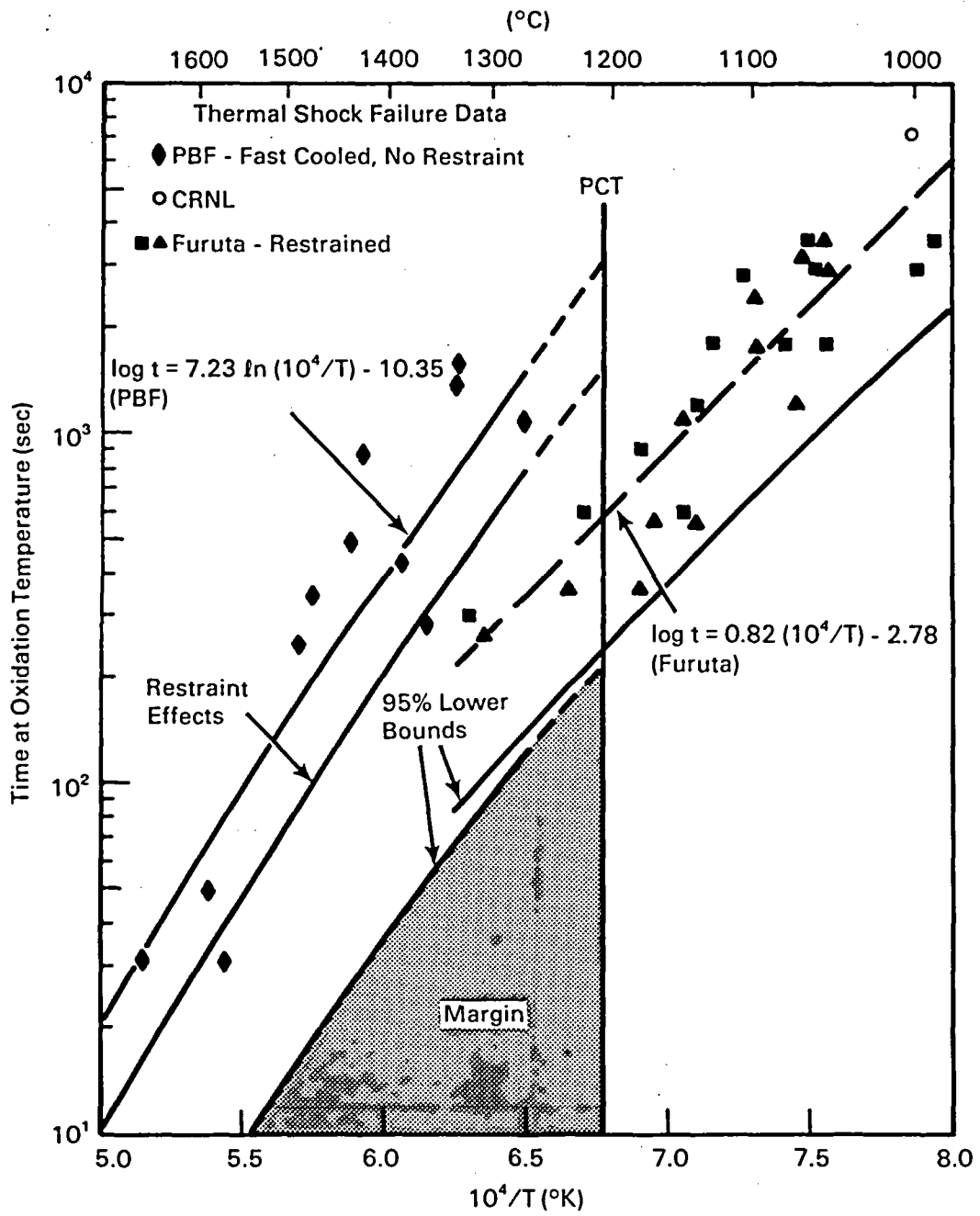


FIGURE 16. PCT Margins for Thermal Shock

bound. It may be of interest to note that the PBF lower bound is nearly identical to the best fit curve for ANL slow cooled data, corrected for cooling rate and axial restraint effects. The latter will be discussed in later paragraphs.

The 95% lower bound in Figure 16 is actually valid only over the range of the PBF data, which do not extend below about 1265°C. The PCT margin for thermal shock appears to vanish at about 210 seconds of oxidation time at 1204°C. This is about the same time anticipated for the maximum duration of a LBLOCA. It was therefore desirable to check this result by comparison with Furuta's [61] data for restrained thermal shock failures at lower temperatures. These data, along with a best fit curve ($r^2 = 0.77$) and 95% lower bound, are also shown in Figure 16. It can be seen that the lower bounds for the two data sets are consistent, even though Furuta's cladding had a wall thickness about 20% greater than in the PBF experiments. Correcting Furuta's data for wall thickness effects would reverse the relative positions of the two lower bounds in Figure 16, while maintaining the same approximate spacing between the bounds in their region of overlap. This is probably not a significant effect, and Furuta's data are considered to confirm the validity of the lower bound estimated from the PBF data. The PCT margin for in-reactor thermal shock is thus represented by the shaded region in Figure 16. This margin is adequate for LBLOCA events, but may not be sufficient for events of longer duration at cladding temperatures approaching 1204°C. The margin for lower temperatures will be addressed in subsequent paragraphs.

PCT Margin for Handling Failures

The ANL [5] and PBF [62] handling failure data are repeated in Figure 17, along with two correlations best fit by the least squares method. The dashed curve was fit to the ANL laboratory data only, with a correlation coefficient of $r^2 = 0.92$. The 95% confidence interval for the next data point, assumed to be a LOCA, is also shown as a dashed curve which passes through the PCT limit at almost the same oxidation time as did the lower bound for the thermal shock data. This lower bound estimate excludes three of the PBF data points from the 95% lower bound confidence interval. This amounts to 3/9 or 33% of the PBF data base, which indicates that the lower bound based on ANL data alone may not be an adequate estimate.

The PBF handling failure data base is so sparse and scattered that a least squares curve fit yielded a line with very low slope and a 95% lower bound that was so minimal that it could not be plotted in Figure 17. It was therefore not possible to use the PBF data alone to produce an estimate of the expected in-reactor handling failure boundary. However, the two data sets appear to present a consistent representation of handling failures in that there is no obvious bias. Also note that it is not necessary to correct the best fit correlations for fast-cooling or axial restraint effects, because the PBF data were fast cooled and there is no restraint effect anticipated for handling failures. Therefore, the two data sets were analyzed as a single data base, and the best fit curve ($r^2 = 0.85$) is shown by the solid line in Figure 17.

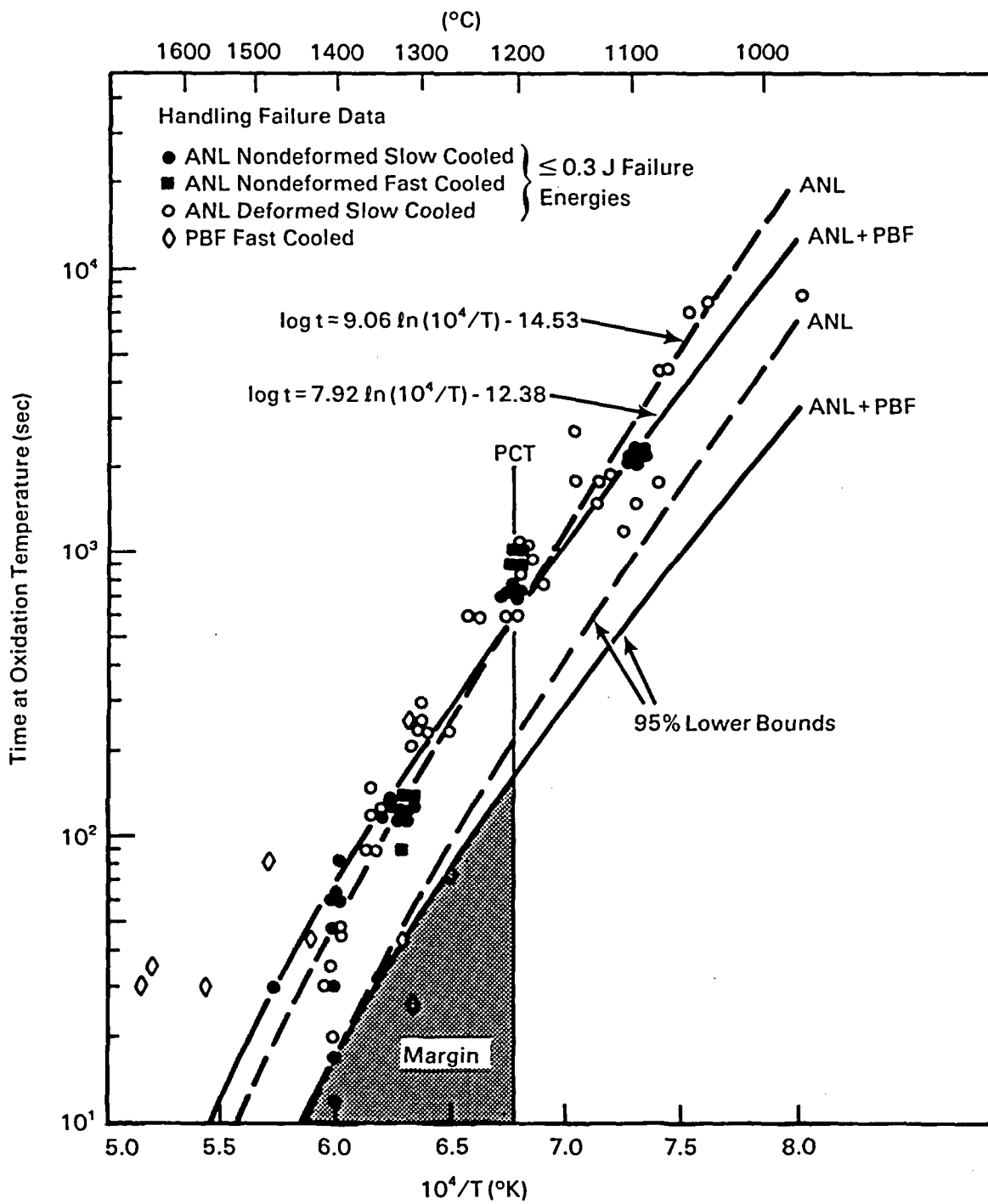


FIGURE 17. PCT Margins for Handling Failures

Note that the two best fit curves cross at about 1250°C, indicating that handling failure correlations are invariant to the above assumption in the vicinity of the PCT limit.

The 95% confidence lower bound for the combined data base is also shown by a solid line in Figure 17, and excludes only one of nine (11%) of the PBF data points. This appears to be a more acceptable estimate of the lowest expected handling failure boundary, and crosses the PCT limit at about 160 seconds of oxidation time, or 76% of the value found for thermal shock failures. The PCT margin for handling failures may therefore be depleted before the end of a LBLOCA if cladding temperatures exceed 1204°C.

Both PCT margins are summarized in Figure 18. It should be restated that these margins are estimated minimum measures of safety over and above the current 1204°C PCT limit, and include estimates of the uncertainties and biases in the data. The effects of cladding deformation (ballooning and rupture), hydrogen absorption, cooling rate, and axial restraint are also included. The margins in Figure 18 were estimated for the case that the next data point to be added to the data base would originate from a power reactor LOCA. With 95% confidence, the margin for that data point would actually be greater than those plotted in Figure 18. At the 67% confidence level, the PCT margins would be roughly twice those shown in Figure 18, as would the times for depletion of the margins. Although this would certainly provide large PCT margins for the LBLOCA, such margins may still be depleted before the end of other LOCA scenarios of much longer duration. However, this is the regime of the 17% ECR limit because temperatures will generally be below 1204°C. ECR margins are discussed in the following paragraphs.

4.2.3 Margins in the ECR Criterion

Thermal shock and handling margins in the 17% ECR limit were assessed using the results of the above analysis. Again, the minimum margins of safety for in-reactor conditions were estimated by subtracting the most limiting case from the estimated lowest bound of the data at a specified confidence limit, assuming that the next data point to be obtained will originate from a LOCA in a power reactor. The "most limiting case" was assumed to occur for two-sided oxidation of cladding that has ballooned and ruptured, since this is thought to occur in the hottest region of the core. The most limiting case is the first to reach 17% ECR at a given temperature. Greater wall thickness or one-sided oxidation require longer times to reach 17% ECR. Margins were estimated for two cases of oxidation rate correlations: the conservative Baker-Just correlation which is currently required by the Criteria, and the "best-estimate" Cathcart-Pawel correlation which closely approaches the mean value of the data base described earlier in this report.

ECR Margin for Thermal Shock

Estimates of the lower bounds for thermal shock failures at the 95% confidence level are shown in Figure 19. The previously published [5,60] ANL curve for slow cooled, non-restrained cladding is shown for reference, along with a

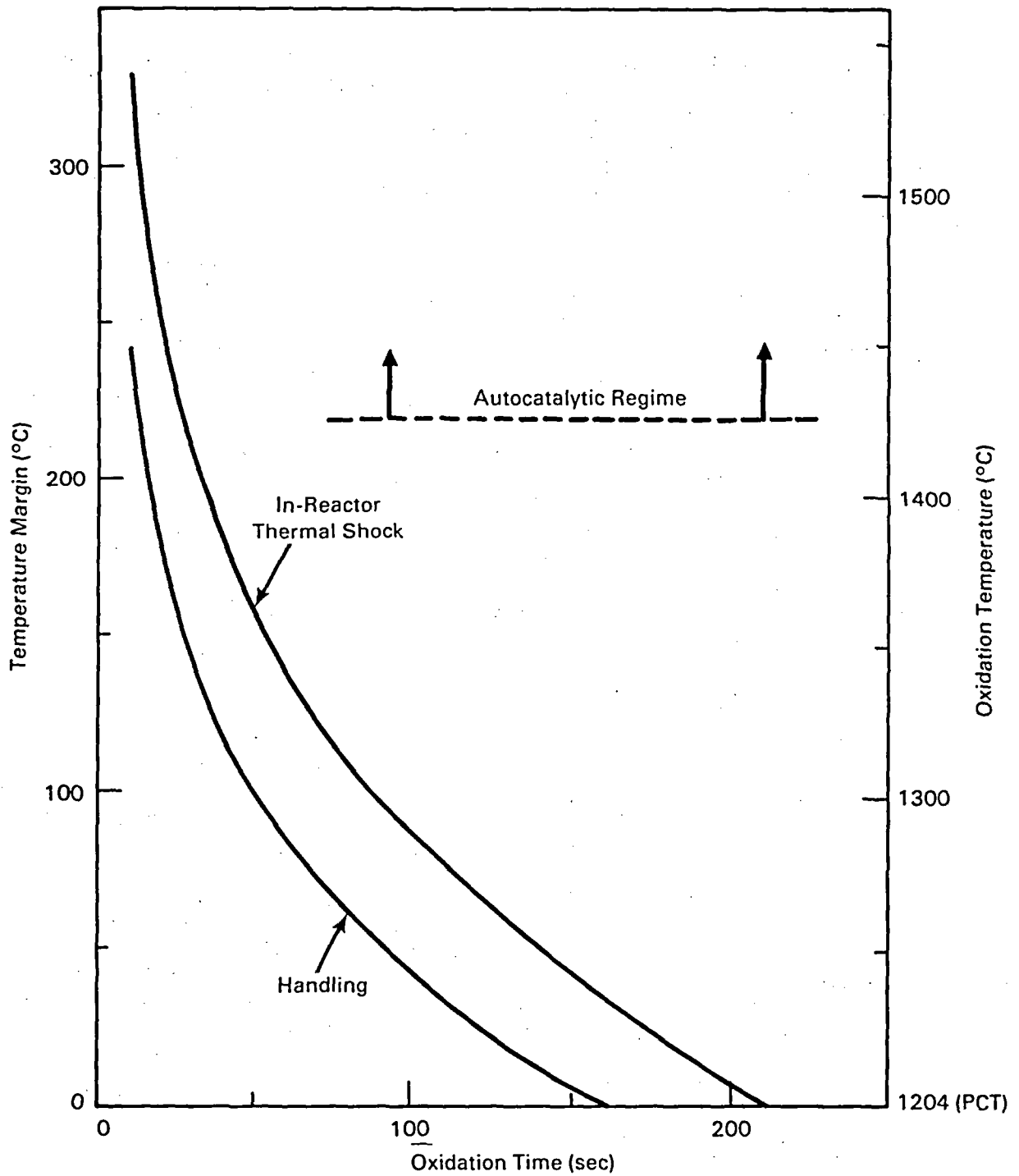


FIGURE 18. Estimated Minimum PCT Margins for Thermal Shock and Handling Failures at the 95% Confidence Level

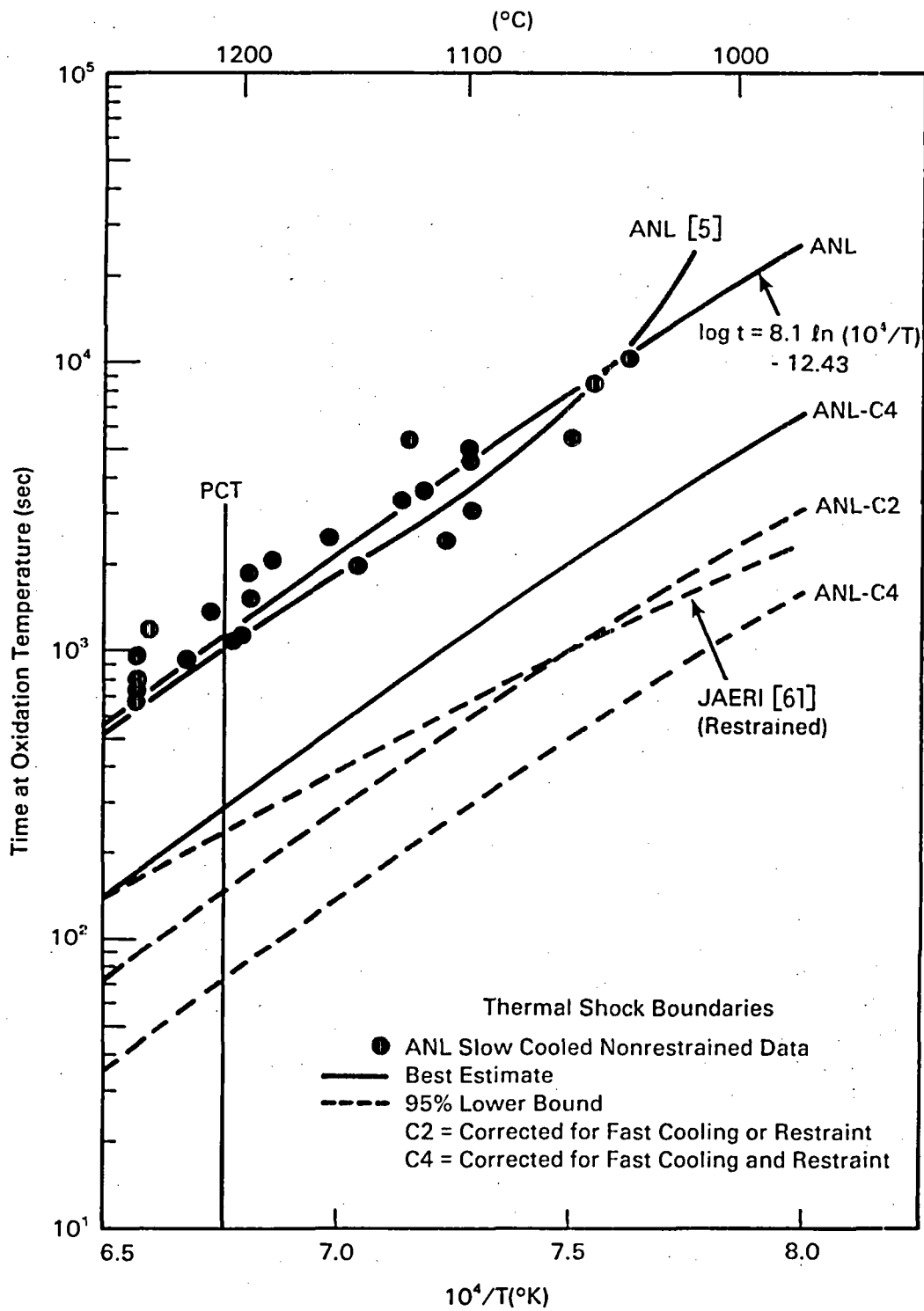


FIGURE 19. Thermal Shock Failure Boundaries at the 95% Confidence Level

curve best fit by the least squares method ($r^2 = 0.83$). The latter curve was developed in the course of estimating the 95% lower bounds. Because this curve represents slow cooled, non-restrained data, corrections must be made to ensure proper representation of the most severe in-reactor conditions. Therefore, the best fit correlation was divided by a factor of four: a factor of two to account for fast cooling effects and another factor of two to account for axial restraint effects. Such effects were described in previous sections of this report. The resulting "corrected" curve is labeled ANL-C4 in Figure 19, as is the corresponding 95% lower bound. For comparison, the 95% lower bound for the ANL curve corrected for only one of the above effects is shown, and is labeled ANL-C2. This curve is somewhat similar to the lowest observed 95% confidence bound from the axially restrained data of Furuta [61]. The ANL-C4 and JAERI [61] lower bounds seem consistent in terms of axial load bearing capability because the cladding wall thickness was about 15% greater in the latter. However, they may be inconsistent in terms of the wall thickness versus thermal shock hoop stress relation.

The 95% lower bound for the ANL-C4 curve is repeated in Figure 20, along with the "most-limiting" curves for 17% ECR. The most limiting cases were computed assuming two sided oxidation of cladding that had been ballooned (32% diametral strain) before rupture. The original wall thickness was chosen as 0.635 mm, the same as the ANL cladding. The time to reach 17% ECR at a given temperature was computed for these cases using the oxidation rate correlations shown in Table 1. It is evident in Figure 20 that the most limiting cases are non-conservative with respect to the 95% lower bound from the ANL-C4 curve. However, some conservatism, or margin, remains at the 50% confidence level. This means that the next data point to be obtained (from a LOCA in a power reactor) will fall above the dashed curve labeled 50%-TS in Figure 20 with 50% probability. This is a significantly smaller confidence interval than previously available, but could still be adequate considering the magnitude of the corrections made above for fast cooling and axial restraint. Note that the conservative Baker-Just oxidation correlation provides a finite margin over the entire temperature range of interest, whereas the margin for the "best-estimate" Cathcart-Pawel correlation vanishes as cladding temperatures exceed about 1160°C. The loss in margin is about 1% ECR at the PCT (1204°C), and could possibly be said to be compensated by the PCT margin itself. However, the ECR and PCT margins are sufficiently different in definition that it should be recognized that the Cathcart-Pawel correlation probably provides no additional margin as temperatures approach 1204°C.

Further definition of "most-limiting" cases is also proper at this point in the discussion. The possibility exists that regions other than the ballooned and ruptured zone may be the most limiting with respect to thermal shock failures. The scenario for this occurrence is as follows. Steam flow through a ballooned (partially blocked) region of the core during a LOCA is a complex process. Ballooning of the cladding provides additional surface area for cooling and may result in a fin cooling effect similar to that observed in the ANL experiments [5]. Flow acceleration through the partially blocked region may further enhance localized cooling. Consequently, the hottest region may occur upstream of the partially blocked region where some degree of flow stagnation may occur. This hotter region then may become the most limiting case. Axial

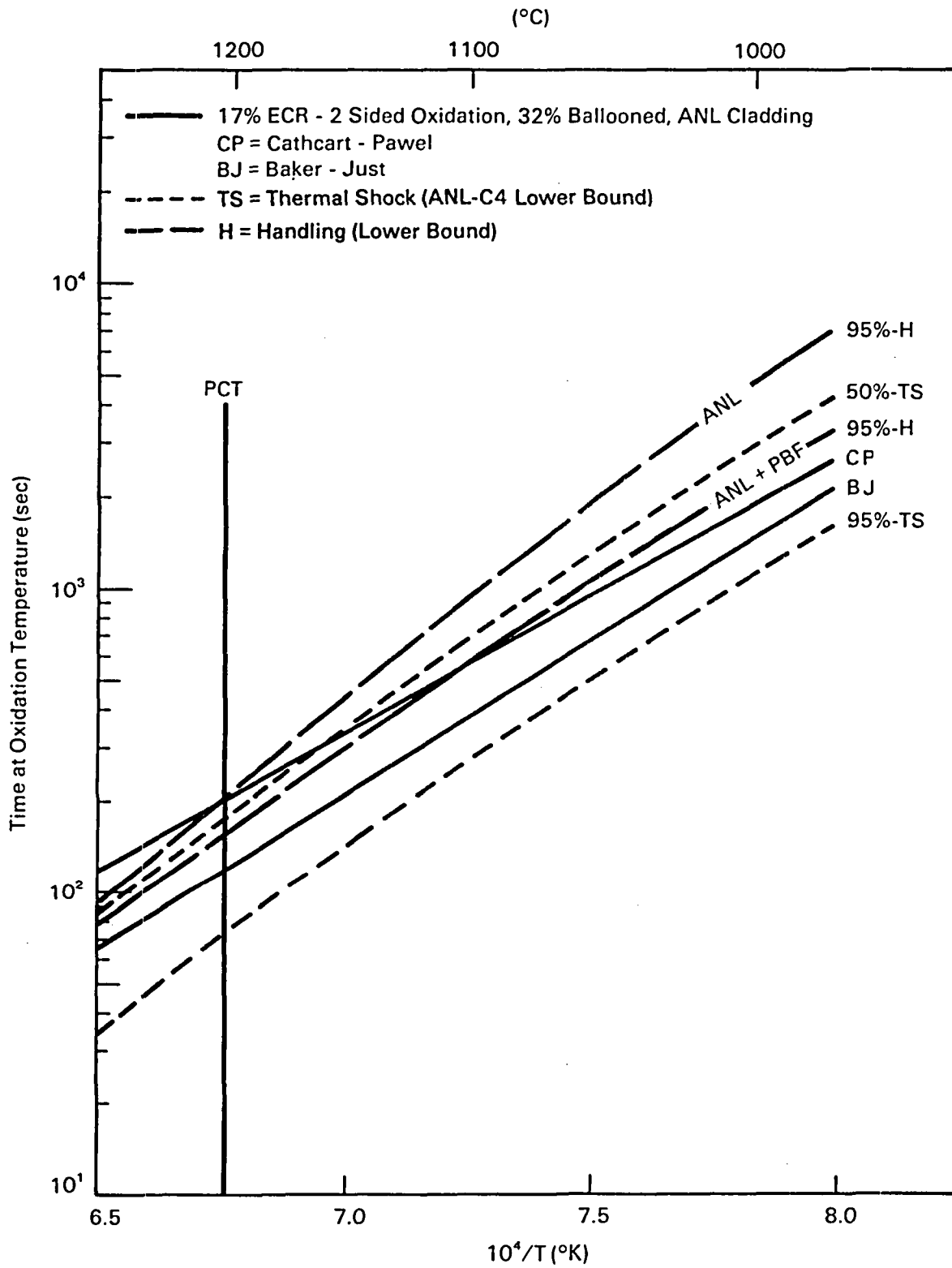


FIGURE 20. Thermal Shock and Handling Failure Boundaries at 50% and 95% Confidence Levels

temperature gradients in the ANL experiments were the cause of failures occurring in nonballooned regions for oxidation temperatures below about 1250°C, and in ballooned regions for temperatures above about 1327°C. Also, Furuta [61] could find no correlation between the extent of oxidation and the axial positions of the thermal shock failures.

Simple calculations show that assuming two-sided oxidation (by virtue of steam ingress) in a non-ballooned region near the rupture opening can produce oxidation comparable to that in the rupture zone itself if the temperatures in the non-ballooned (stagnation) zone are as little as 40 to 70°C higher than in the ballooned/ruptured zone. Axial temperature gradients of 160-180°C were noted in the ANL experiments, and have been observed in the NRII LOCA simulations [69]. It appears possible that the increased understanding of core conditions during a LOCA, acquired in the last decade, may in turn result in a need for improved definition of the "most-limiting" case before changes are made in the Criteria. In particular, the relation between fracture mode and axial location, metallurgical condition of ballooned versus non-ballooned regions, and axial restraint versus thermal shock hoop loads should be further investigated. Although thermal shock loadings were addressed at the time of the hearings, the Commission did not feel that a sufficient basis existed for incorporation of these effects into the criteria in a quantitative manner. The subject has apparently been largely neglected since that time, despite advances in both fracture technology and the LOCA-related data base [i.e., 70-72] which make such an analysis possible.

ECR Margin for Handling Failures

The lower bounds for handling failures at the 95% confidence level are also shown in Figure 20. The upper curve is for the ANL data only, and is for failures under impact loadings of less than or equal to 0.3J. The lower curve is for the combined ANL and PBF handling failure data base. Both curves are reproduced from Figure 17. It could be argued that the upper curve (ANL data only) should be used to assess ECR handling failure margins because there were no in-reactor (PBF) data below the PCT. However, for consistency in this analysis, the ANL+PBF curve was used because it yields the lowest bound, and provides the smallest expected margin. It can be seen in Figure 20 that use of the Baker-Just correlation results in adequate margins over the entire range of temperatures. However, use of the Cathcart-Pawel correlation results in a vanishing margin for temperatures above about 1100°C. It would again appear that use of the best estimate oxidation correlation results in loss of the minimum expected ECR margin for handling failures at the 95% confidence level, and thus that further analyses should be conducted before changes in the Criteria are finalized. The results of the above ECR margin analyses are summarized in Figure 21.

Alternative Analysis of ECR Margins

The above analysis indicates a possible lack of justification for replacing the currently required Baker-Just correlation with the "best-estimate" Cathcart-Pawel oxidation rate equation for temperatures below 1204°C,

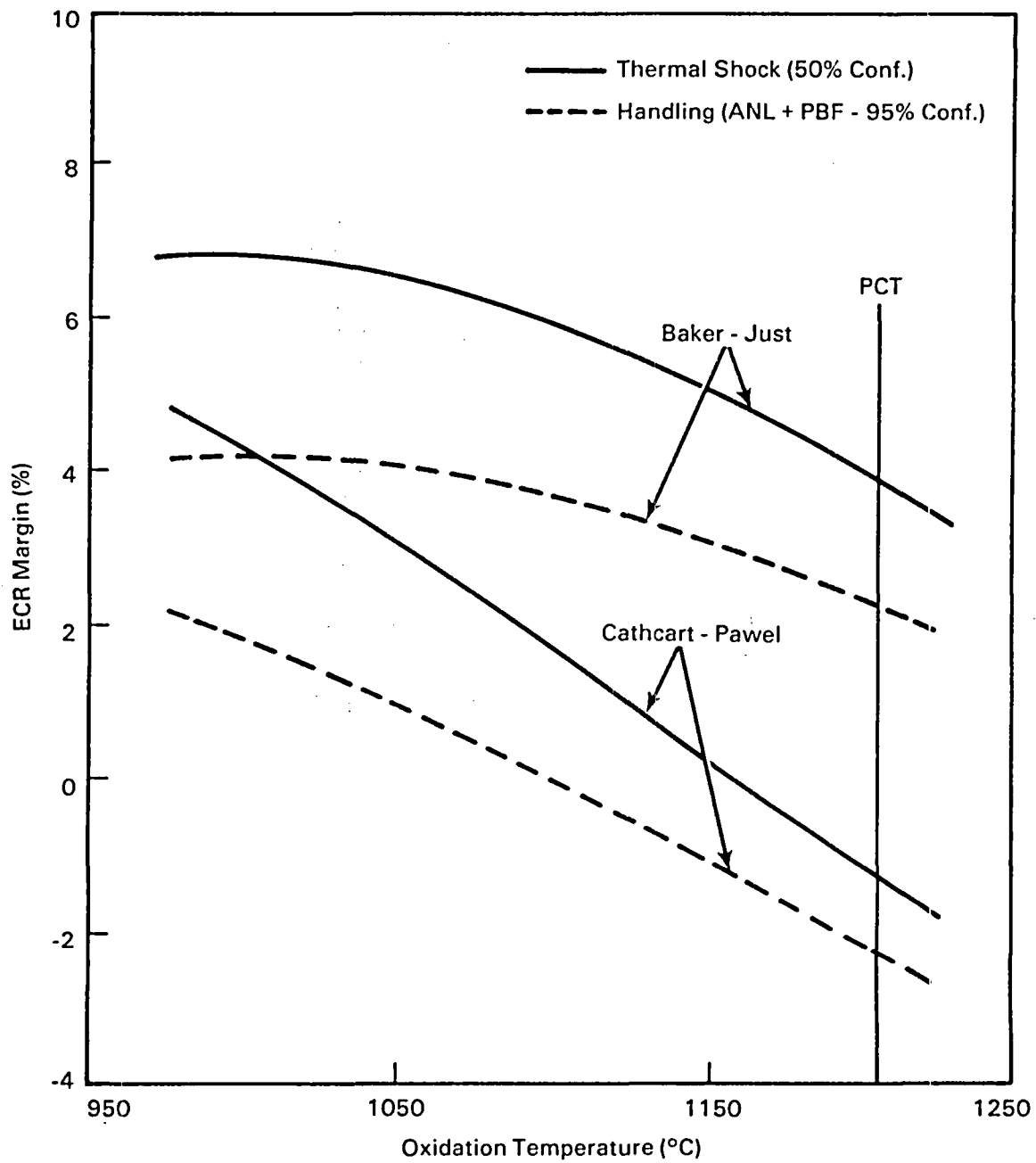


FIGURE 21. Minimum ECR Margins for Thermal Shock and Handling Failures

whereas the analysis in Section 4.1 implied that such a replacement seemed justified. This apparent contradiction can be resolved with an alternative set of assumptions for the ECR margin analysis, as follows.

It must be assumed that the ANL-C2 curve in Figure 19 adequately represents the 95% lower bound for thermal shock failures. Use of this assumption is dependent upon showing that either (1) fast cooling effects are negligible because slow cooling is expected due to decay heat considerations, or (2) axial restraint renders cooling rate effects negligible. The latter condition is supported by Furuta's [61] axially restrained data, shown most clearly in Figure 16. Comparison with Figure 20 shows that the ANL-C2 curve very nearly coincides with the 95% lower bound for handling failures using the combined ANL+PBF data base. Margins for ECR thermal shock and handling failures will therefore be nearly identical, which is generally not the case in previous investigations [5,60].

Figure 20 indicates that ECR margins still vanish above 1100°C for the Cathcart-Pawel limiting case. The ANL+PBF and ANL-C2 lower boundaries must be moved upward in order to provide ECR margins for all temperatures below the 1204°C PCT. In other words, the lower boundaries must pass through the Cathcart-Pawel/PCT intersection point in Figure 20, at about 200 seconds oxidation time. This is possible by reducing the confidence levels to 85% for thermal shock and 88% for handling failures. These confidence levels seem entirely sufficient to justify the use of the Cathcart-Pawel oxidation equation in LOCA calculations, provided that the above assumptions are acceptable.

5.0 SUMMARY AND CONCLUSIONS

The ECCS Acceptance Criteria include specifications concerning Zircaloy-steam oxidation rate equations (the Baker-Just correlation), the maximum allowable cladding temperature (1204°C PCT), and the maximum allowable oxidation of the cladding (17% ECR) to be permitted during a LOCA. These criteria were instituted over a decade ago and were intended to yield conservative estimates of cladding performance during a LOCA, thus providing an additional safety margin over and above the expected uncertainties in the data base. Research performed since that time has improved that data base to the extent where those safety margins can be assessed quantitatively.

Such an analysis is described in this report. The general approach was to use the current (1985) data base to statistically estimate the most extreme values expected at the 95% confidence level for oxidation rate constants and for cladding failure properties under thermal shock and handling conditions. The margin of safety was defined as the difference between the estimated extreme value and the value of the criterion, i.e., maximum expected oxidation rate minus that predicted by the Baker-Just correlation, or minimum oxidation time for failure by thermal shock minus the time to reach 17% ECR at the same temperature. It is important to realize that the margins so estimated are the minimum expected margins at the specified confidence level.

The maximum expected values for oxidation rate constants were estimated at the 95% confidence level for the substantial data base available using standard statistical methods. High pressure steam was the only factor found to possibly increase the maximum expected oxidation rates above the 95% boundary in the 1000-1500°C temperature regime. This occurs only over the range of a phase transformation in the generally protective oxide layer on the cladding surface (950-1100°C). However, the safety margin for the conservative Baker-Just correlation vanishes below about 1100°C, so the effects of high pressure steam are also inconsequential. The minimum expected margin in the oxidation rate constant rises from zero at 1100°C to 105% at 1500°C, but again vanishes at higher temperatures (-22% at 1510°C and -40% at 1900°C). Maximum oxidation rate constants for the 1500-2000°C temperature range may be slightly increased by saturation of the beta phase, but the negative margin for the Baker-Just correlation was dominated by scatter in the data base itself.

The Baker-just correlation thus yields positive margins only over the 1100-1500°C temperature range. The inconsistent margins in this currently specified oxidation rate correlation appear to indicate that alternative rate equations may be a viable consideration for future revisions in the ECCS Acceptance Criteria. However, this will place more importance on margins in the embrittlement criteria.

Margins in the Zircaloy-steam embrittlement criteria (1204°C PCT, 17% ECR) were assessed using both laboratory and in-reactor data which simulated fuel rods, so that the effects of ballooning and rupture, two-sided oxidation, and hydrogen absorption are implicit in the data base. The effects of fast cooling rates and axial restraints were estimated for in-reactor conditions, and were

found to decrease the allowable oxidation times to failure by about a factor of two each. The lowest expected boundaries for thermal shock and handling failures were estimated from the data base assuming that the next data point to be added to the data base would originate from a LOCA in a commercial reactor. The statistical method employed resulted in lower bounds which represent 95% certainty that this next data point will fall above the failure boundaries, with margins greater than those estimated herein.

The minimum expected PCT margin at the 95% confidence level for thermal shock was found to be quite substantial for brief oxidation times above 1204°C, i.e., less than 100 seconds. This margin fell to zero at about 210 seconds, which is comparable to the anticipated duration of a LBLOCA. The PCT margin for handling failures followed a similar trend at the 95% confidence level, but vanished at about 160 seconds, so that the minimum margin may be depleted before the end of a LBLOCA.

Margins in the ECR were estimated assuming that the most limiting in-core oxidation condition occurred at the ballooned and ruptured region, which reaches 17% ECR in the shortest time. Recent data may indicate that this assumption should be questioned. The minimum expected ECR margin for thermal shock did not exist at the 95% confidence level. At the 50% confidence level, the conservative Baker-Just correlation provides a 4% to 7% ECR margin for thermal shock, while the best-estimate Cathcart-Pawel correlation provides about a 4% ECR thermal shock margin at 1000°C which vanishes at about 1160°C. The minimum expected ECR margins for handling failures were specified by laboratory impact tests at 0.3J or less at room temperature and by in-reactor data. At the 95% confidence level, the Baker-Just correlation provides a 2% to 4% margin for handling failures, while the Cathcart-Pawel correlation provides about a 2% ECR margin at 1000°C which vanishes at about 1100°C. Assuming that the 50% confidence level is acceptable for thermal shock failures, ECR margins may thus be adequate for calculations performed with the currently required Baker-Just oxidation correlation, but may be insufficient for the best-estimate Cathcart-Pawel correlation. An alternative analysis of ECR margins was found to provide justification for use of the Cathcart-Pawel relation at about the 85-88% confidence level, if the effects of cooling rate can be discounted.

Note that these are minimum expected margins at specified confidence levels, and were estimated from the failed data only. The present analysis may be improved by employing statistical techniques which utilize the entire data base (failed and non-failed) to better define the failure boundaries via logistic regression methods [67]. This may provide additional margins. The general results of the present analysis seem somewhat contradictory. Revision of the oxidation rate equation requirements to permit use of best-estimate correlations is indicated. This does not affect the PCT margin, but may yield insufficient ECR margins. However, these criteria have generally been found to be conservative in other analyses [3,5,6] using more sophisticated methods to simulate the oxidation reaction [73-75]. It is believed that an analysis of Zircaloy fracture behavior incorporating the best available mechanistic oxidation codes described in [73-75] will reveal that sufficient margin in fact does exist for simplified LOCA calculations based on the best-estimate Cathcart-Pawel correlation.

6.0 REFERENCES

1. U.S. Code of Federal Regulations, Title 10, Part 50.46 and Appendix K.
2. H. Bethe, et al., "Report to the American Physical Society by the Study Group on Light-Water Reactor Safety." Rev. Mod. Phys, Vol. 47, Suppl. No. 1, 1975.
3. C. A. Mann, et al., "Deformation of PWR Fuel in a Loss-of-Coolant Accident (LOCA)," UKAEA, Springfields Nuclear Power Establishment, CSNI Paper, 1985.
4. D. A. Powers and R. O. Meyer, "Cladding Swelling and Rupture Models for LOCA Analysis," NUREG-0630, April 1980.
5. H. M. Chung and T. F. Kassner, "Embrittlement Criteria for Zircaloy Fuel Cladding Applicable to Accident Situations in Light-Water Reactors: Summary Report," NUREG/CR-1344, ANL-79-48, January 1980.
6. A. W. Lemmon, "Studies Relating to the Reaction Between Zirconium and Water at High Temperature," BMI-1154, 1957.
7. W. A. Bostrum, "The High Temperature Oxidation of Zircaloy in Water," WAPD-104, 1954.
8. L. Baker and L. C. Just, "Studies of Metal-Water Reactions at High Temperature: III. Experimental and Theoretical Studies of Zirconium-Water Reaction," ANL-6548, 1962.
9. D. O. Hobson and P. L. Rittenhouse, "Embrittlement of Zircaloy-Clad Fuel Rods by Steam During LOCA Transients," ORNL-4758 January 1972.
10. R. E. Pawel, "Oxygen Diffusion in Beta Zircaloy During Steam Oxidation." J. of Nucl. Mater. 50 247-258, 1974.
11. Letter Report from D. B. Trauger, ORNL, to J. H. Hendrie, AEC, January 30, 1973, "Consulting with the AEC Regulatory Staff on Oxidation and Embrittlement," Task 2 "Calculate Oxidation Rates from Penetration Data to Compare Statistically with the Baker-Just Rate Data," page 6.
12. United States Atomic Energy Commission Docket No. RM-50-1, December 1973, "Opinion of the Commissioners," p. 56, 57, 58.
13. J. C. Hesson, R. O. Ivins, R. E. Wilson, K. Nishino and C. Barnes, "Laboratory Simulations of Cladding Steam Reactions Following Loss of Coolant Accidents in Water Cooled Reactors," ANL-7609, January 1970.
14. J. D. Duncan and J. E. Leonard, "Thermal Response and Cladding Performance of Zircaloy Clad Simulated Fuel Bundles Under High Temperature Loss of Coolant Conditions," GEAP-13174, General Electric Company, May 1971.

15. G. J. Scatena, "Fuel Cladding Embrittlement During a Loss of Coolant Accident," NEDO-10674, General Electric Company, October 1972.
16. R. H. Meservey and R. Henzel, "Embrittlement Behavior of Zircaloy in an Emergency Core Cooling Environment," IN-1389, Idaho Nuclear Corporation, September 1970.
17. D. O. Hobson, "Ductile-Brittle Behavior of Zircaloy Fuel Cladding," Proc. ANS Topical Meeting on Water-Reactor Safety, CONF-730304, pp. 274-288, 1973.
18. P. D. Parsons, "A Review of the Diffusion Coefficients of Oxygen in α and β Zirconium Alloys in the Temperature Range 675-1800°C." UKAEA Report TRG 2882(S), January 1977.
19. R. E. Pawel, "Oxygen Diffusion in the Oxide and Alpha Phases During Reaction of Zircaloy-4 with Steam from 1000° to 1500°C." J. Electrochem. Soc. Vol. 126, No. 7, 1979, pp. 1111-1118.
20. H. M. Chung and T. F. Kassner, "Pseudo Binary Zircaloy-Oxygen Phase Diagram," J. Nucl. Mater. 84, 1979, p. 327.
21. R. R. Biederman, et al., "A Study of Zircaloy-4 Steam Oxidation Reaction Kinetics" EPRI-NP-225, Final Report, September 1976.
22. J. V. Cathcart and R. E. Pawel, "Zirconium Metal-Water Oxidation Kinetics: IV. Reaction Rate Studies." ORNL/NUREG-17, August 1977.
23. R. E. Westerman and G. M. Hesson, "Zircaloy Cladding i.d./o.d. Oxidation Studies." EPRI NP-525 Final Report, November 1977.
24. R. R. Biederman, R. D. Sisson, J. K. Jones, and W. G. Dobson, "A Study of Zircaloy-4 - Steam Oxidation Reaction Kinetics." EPRI NP-734, Final Report, April 1978.
25. S. Kawasaki, T. Furuta, and M. Suzuki, "Oxidation of Zircaloy-4 Under High Temperature Steam Atmosphere and Its Effect on Ductility of Cladding." J. Nucl. Sci. Technol., Vol. 15, No. 8, 1978, pp. 589-596.
26. S. Kawasaki, et al., "Oxidation of Zircaloy-4 Under High Temperature Steam Atmosphere and Its Effect on Ductility of Cladding." J. Nucl. Sci. Tech., Vol. 15 No. 8, August 1978, pp. 589-596.
27. V. F. Urbanic and T. R. Heidrick, "High-Temperature Oxidation of Zircaloy-2 and Zircaloy-4 in Steam." J. Nucl. Mater., Vol. 75, No. 2, 1978, pp. 251-261.
28. S. Leistikow, G. Schanz, and H. v. Berg, "Kinetics and Morphology of Isothermal Steam Oxidation of Zircaloy-4 at 700-1300°C." KFK 3587, March 1978.

29. A. F. Brown and T. Healey, "The Kinetics of Total Oxygen Uptake in Steam-Oxidized Zircaloy-2 in the Range 1273-1673K." J. Nucl. Mater., Vol. 88, No. 1, 1980, pp. 1-6.
30. H. M. Chung and G. R. Thomas, "Zircaloy Oxidation and Hydrogen Generation Rates in Degraded Core Accident Conditions." International Workshop on the Impact of Hydrogen on Water Reactor Safety, Albuquerque, New Mexico, USA, October 1982.
31. A. E. Aly, "Oxidation of Zircaloy-4 Tubing in Steam at 1350 to 1600°C." KFK-3358, May 1982.
32. S. Leistikow, G. Schanz, H. v. Berg, and A. E. Aly, "Comprehensive Presentation of Extended Zircaloy-4 Steam Oxidation Results (600-1600°C)." OECD-NEA-CSNI/IAEA Specialists Meeting on Water Reactor Fuel Safety and Fission Product Release in Off-Normal and Accident Conditions, Risø, May 1983.
33. J. T. Prater and E. L. Courtright, "Oxidation of Zircaloy-4 in Steam at 1300 to 2400°C," PNL-SA-13122, Presented at the 7th International Conference on Zirconium in the Nuclear Industry, Salzburg, France, June 24-27, 1985.
34. B. Cox, "Oxidation of Zirconium and Its Alloys." Advances in Corrosion Science and Technology, Plenum Press, 1976.
35. G. Schanz and S. Leistikow, "ZrO₂-Scale Degradation During Zircaloy-4 High Temperature Steam Exposure, Microstructural Mechanisms and Consequences for PWR Safety Analysis," Proc. ANS/ENS Topical Meeting on Reactor Safety Aspects of Fuel Behavior, Sun Valley USA, August 1981.
36. A. B. Johnson, "Effects of Nuclear Radiation on the Corrosion, Hydriding and Oxide Properties of Six Zirconium Alloys." ASTM STP-458, p. 301.
37. R. C. Asher, "The Effect of Radiation on the Aqueous Corrosion of Zircaloy. A Survey of World Experience." UKAEA Report AERE-R-7454, 1973.
38. S. Hagen, et al., "Temperature Escalation in PWR Fuel Rod Simulators Due to the Zircaloy-Steam Reaction: ESSI-4 to ESSI-11 Test Results Report," KFK-3557, March 1985.
39. R. E. Pawel and J. J. Campbell, "The Observation of Effects of Finite Specimen Geometry on the Oxidation Kinetics of Zircaloy-4." J. Electrochem. Soc. Vol. 127, No. 10, 1980, pp. 2188-2194.
40. C. F. Knights and R. Perkins, "The Effect of Applied Tensile Stress on the Corrosion Behavior of Zircaloy-2 in Steam." J. Nucl. Mater., Vol. 36, 1970, pp. 180-188.

41. D. H. Bradhurst and P. M. Heuer, "The Effects of Deformation on the High Temperature Steam Oxidation of Zircaloy-2." *J. Nucl. Mater.*, Vol. 55, 1975, pp. 311-326.
42. S. Leistikow and R. Kraft, "Creep Rupture Testing of Zircaloy-4 Tubing Under Superimposed High Temperature Steam Oxidation at 900°C." *Proc. Sixth European Congress on Metallic Corrosion*, London, Sept. 1977.
43. T. Furuta and S. Kawasaki, "Acceleration of Zircaloy-Steam Reaction Rate by Deformation Under High Temperature Transient." *J. Nucl. Sci. Technol.*, Vol. 17, No. 3, 1980, pp. 243-245.
44. A. T. Donaldson and H. E. Evans, "Oxidation Induced Creep in Zircaloy-2: I, II, III." *J. Nucl. Mater.*, Vol. 99, 1981, pp. 38-65.
45. J. V. Cathcart, et al. "Zirconium Metal-Water Oxidation Kinetics. IV. Reaction Rate Studies," ORNL/NUREG-17, 1977, pp. 85-93.
46. S. Leistikow, R. Kraft, and E. Pott, "Is Air a Suitable Environment for Simulation of Zircaloy-Steam High Temperature Oxidation Within Engineering Experiments." EUR 6984, 1981.
47. R. E. Pawel, J. V. Cathcart, and J. J. Campbell, "The Oxidation of Zircaloy-4 at 900 and 1100°C in High Pressure Steam." *J. Nucl. Mater.*, Vol. 82, No. 1, 1979, pp. 129-139.
48. R. E. Westerman, "High Temperature Oxidation of Zirconium and Zircaloy-2 and Oxygen or Water Vapor," HW-73511, 1962.
49. T. Furuta, et al., "Deformation and Inner Oxidation of the Fuel Rod in a Loss-of-Coolant Accident Condition." JAERI-M-6339, NRC Translation NR-TR-005, 1975.
50. T. Furuta, et al., "Zircaloy Clad Fuel Rod Burst Behavior Under Simulated Loss-of-Coolant Conditions in PWRs." *J. Nucl. Sci. Technol.*, Vol. 15, No. 10, 1978, pp. 736-744.
51. S. Kawasaki, et al., "Inner Surface Oxidation of Zircaloy Cladding in a Loss-of-Coolant Accident." Presented at the Sixth Water Reactor Safety Research Information Meeting, Gaithersburg, USA November 1978.
52. H. Uetsuka, et al., "Zircaloy-4 Cladding Embrittlement Due to Inner Surface Oxidation Under Simulated Loss-of-Coolant Condition." *J. Nucl. Sci. Technol.*, Vol. 18, No. 19, 1981, pp. 705-717.
53. T. Furuta, et al., "Ductility Loss of Zircaloy Cladding by Inner Surface Oxidation During High Temperature Transient." *J. Nucl. Sci. Technol.*, Vol. 18, No. 20, 1981, pp. 802-810.

54. K. Homma, et al., "Behavior of the Zircaloy Cladding Tube in a Mixed Gas of Hydrogen and Steam", JAERI M-7131, 1977. NRC Translation NUREG/TR-0021.
55. T. Furuta, et al., "Reaction Behavior of Zircaloy-4 in Steam Hydrogen Mixtures at High Temperature," J. Nucl. Sci. Technol., Vol. 105, 1982, pp. 1119-1131.
56. H. Uetsuka, "Oxidation of Zircaloy-4 Under Limited Steam Supply at 1000 and 1300°C," KfK (Kernforschungszentrum Karlsruhe, Germany) Report 3848, December 1984.
57. H. M. Chung and G. R. Thomas, "Rate Limiting Effects of Gaseous Hydrogen on Zircaloy Oxidation." NRC Workshop on the Impact of Hydrogen on Water Reactor Safety, Albuquerque, New Mexico, USA, January 1981.
58. H. M. Chung and G. R. Thomas, "High Temperature Oxidation of Zircaloy in Hydrogen-Steam Mixtures." Paper Presented at the 6th International Conference on Zirconium in the Nuclear Industry, Vancouver, B.C., Canada, June 1982.
59. L. Baker, Jr, "An Assessment of Existing Data on Zirconium Oxidation Under Hypothetical Accident Conditions in Light-Water Reactors," ANL/LWR/SAF-83-3, 1983.
60. R. Van Houten. "Fuel Rod Failure as a Consequence of Departure from Nucleate Boiling or Dryout," NUREG-0562, June 1979.
61. T. Furuta, et al., "Estimation of Conservatism of Present Embrittlement Criteria for Zircaloy Fuel Cladding Under LOCA," in Zirconium in the Nuclear Industry: 6th International Symposium, ASTM STP-824, D. G. Franklin and R. B. Adamson, eds., Am. Soc. for Testing and Mater., 1984, pp. 734-746.
62. F. M. Haggag, "Zircaloy Cladding Embrittlement Criteria: Comparison of In-Pile and Out-of-Pile Results," NUREG/CR-2757, July 1982.
63. S. Shiozawa, et al., "Evaluation on Oxidation of Zircaloy-4 During Rapid Transient in NSRR Experiments." JAERI-M-8187, March 1979.
64. T. Hoshi, et al., "Fuel Failure Behavior of PCI-Remedy Fuels Under Reactivity Initiated Accident Conditions." JAERI-M-8836, May 1980.
65. Anonymous, "Semiannual Progress Report on the NSRR Experiments - July to December 1979." JAERI-M-9011, September 1980.
66. T. Fujishiro, et al., "The Influence of Coolant Flow on Fuel Behavior Under Reactivity Initiated Accident Conditions." JAERI-M-9104, October 1980.

67. R. L. Wine, "Statistics for Scientists and Engineers," Prentice-Hall, Inc., Englewood Cliffs, New Jersey, 1964.
68. G. J. Lieberman, et al., "Unlimited Simultaneous Discrimination Intervals in Regression," *Biometrika*, Vol. 54, Nos. 1 and 2, 1967, pp. 133-145.
69. C. L. Wilson, et al., "LOCA Simulation in NRU Program: Data Report for the Fourth Materials Experiment (MT-4)," NUREG/CR-3272, PNL-4669, May 1983.
70. R. H. Chapman, et al., "Zirconium Cladding Deformation in a Steam Environment with Transient Heating" in *Zirconium in the Nuclear Industry (4th Conference)*, J. H. Schemel and T. P. Papazesglou, eds. ASTM STP-681, Amer. Soc. for Testing and Mater., 1979, pp. 393-488.
71. A. Sawatsky, G. A. Ledoux, and S. Jones, "Oxidation of Zirconium During a High Temperature Transient." in *Zirconium in the Nuclear Industry*, ASTM STP-633, A. L. Lowe, Jr. and G. W. Parry, Editors (1977), pp. 143-149.
72. S. L. Sieffert, "The Effect of Hydrogen on the Oxygen Embrittlement of Beta-Quenched Zircaloy Fuel Cladding." in *Zirconium in the Nuclear Industry (Fifth Conference)*, D. G. Franklin, ed., ASTM STP-754. January 1982, pp. 302-328.
73. S. Malang, "SIMTRAN-1: A Computer Code for the Simultaneous Calculation of Oxygen Distribution and Temperature Profiles in Zircaloy During Exposure to High Temperature Oxidizing Environments," ORNL-5083, November 1975.
74. W. G. Dobson and R. R. Biederman, "ZORO-1: A Finite Difference Computer Model for Zircaloy-4 Oxidation in Steam." EPRI-NP-347, December 1976.
75. M. Suzuki and S. Kawasaki, "Development of Computer Code PRECIP-II for Calculations of Zr Steam Reaction." *J. Nucl. Sci. Technol.* Vol. 17, No. 4, 1980, pp. 291-300.

DISTRIBUTION

No. of
Copies

No. of
Copies

OFFSITE

U.S. Nuclear Regulatory
Commission
Division of Technical
Information and Document
Control
7920 Norfolk Avenue
Bethesda, MD 20014

D. F. Ross
U.S. Nuclear Regulatory
Commission
M/S 1130-SS
Washington, DC 20555

M. Silberberg
U.S. Nuclear Regulatory
Commission
M/S 1130-SS
Washington, DC 20555

G. Marino
U.S. Nuclear Regulatory
Commission
M/S 1130-SS
Washington, DC 20555

R. Lobel
Reactor Systems Branch
Division of PWR Licensing-A
Office of Nuclear Reactor
Regulation
U.S. Nuclear Regulatory
Commission
Washington, DC 20555

10 R. Van Houten
Fuel Systems Research Branch
Division of Accident Evaluation
U.S. Nuclear Regulatory
Commission
Washington, DC 20555

ONSITE

19 Pacific Northwest Laboratory

W. J. Bailey
C. E. Beyer
M. D. Freshley
G. M. Hesson
D. D. Lanning
F. E. Panisko
J. T. Prater
R. E. Williford (5)
Technical Information (5)
Publishing Coordination (2)



NRC FORM 335 (2-84) NRCM 1102, 3201, 3202 SEE INSTRUCTIONS ON THE REVERSE	U.S. NUCLEAR REGULATORY COMMISSION BIBLIOGRAPHIC DATA SHEET	1. REPORT NUMBER (Assigned by TICC, add Vol. No., if any) NUREG/CR-4412 PNL-5601				
2. TITLE AND SUBTITLE An Assessment of Safety Margins in Zircaloy Oxidation and Embrittlement Criteria for ECCS Acceptance	3. LEAVE BLANK					
5. AUTHOR(S) R. E. Williford	4. DATE REPORT COMPLETED <hr/> <table style="width:100%; border: none;"> <tr> <td style="text-align: center; border: none;">MONTH</td> <td style="text-align: center; border: none;">YEAR</td> </tr> <tr> <td style="text-align: center; border: none;">November</td> <td style="text-align: center; border: none;">1985</td> </tr> </table>		MONTH	YEAR	November	1985
MONTH	YEAR					
November	1985					
7. PERFORMING ORGANIZATION NAME AND MAILING ADDRESS (Include Zip Code) Pacific Northwest Laboratory P.O. Box 999 Richland, WA 99352	6. DATE REPORT ISSUED <hr/> <table style="width:100%; border: none;"> <tr> <td style="text-align: center; border: none;">MONTH</td> <td style="text-align: center; border: none;">YEAR</td> </tr> <tr> <td style="text-align: center; border: none;">April</td> <td style="text-align: center; border: none;">1986</td> </tr> </table>		MONTH	YEAR	April	1986
MONTH	YEAR					
April	1986					
10. SPONSORING ORGANIZATION NAME AND MAILING ADDRESS (Include Zip Code) Division of Accident Evaluation Office of Nuclear Regulatory Research U.S. Nuclear Regulatory Commission Washington, D.C. 20555	8. PROJECT/TASK/WORK UNIT NUMBER <hr/> 9. FIN OR GRANT NUMBER B2277					
12. SUPPLEMENTARY NOTES	11a. TYPE OF REPORT <hr/> b. PERIOD COVERED (Inclusive dates)					
13. ABSTRACT (200 words or less) Current Emergency Core Cooling System (ECCS) Acceptance Criteria for light-water reactors include certain requirements pertaining to calculations of core performance during a Loss of Coolant Accident (LOCA). The Baker-Just correlation must be used to calculate Zircaloy-steam oxidation, calculated peak cladding temperatures (PCT) must not exceed 1204°C, and calculated oxidation must not exceed 17% equivalent cladding reacted (17% ECR). The minimum margin of safety was estimated for each of these criteria, based on research performed in the last decade. Margins were defined as the amounts of conservatism over and above the expected extreme values computed from the data base at specified confidence levels. The currently required Baker-Just oxidation correlation provides margins only over the 1100°C to 1500°C temperature range at the 95% confidence level. The PCT margins for thermal shock and handling failures are adequate at oxidation temperatures above 1204°C for 210 and 160 seconds, respectively, at the 95% confidence level. ECR thermal shock and handling margins at the 50% and 95% confidence levels, respectively, range between 2% and 7% ECR for the Baker-Just correlation, but vanish at temperatures between 1100°C and 1160°C for the best-estimate Cathcart-Pawel correlation. Use of the Cathcart-Pawel correlation for LOCA calculations can be justified at the 85% to 88% confidence level if cooling rate effects can be neglected.						
14. DOCUMENT ANALYSIS - a. KEYWORDS/DESCRIPTORS ECCS Acceptance Criteria Zircaloy Oxidation and Embrittlement Safety margins b. IDENTIFIERS/OPEN-ENDED TERMS	15. AVAILABILITY STATEMENT Unlimited 16. SECURITY CLASSIFICATION <hr/> <i>(This page)</i> Unclassified <hr/> <i>(This report)</i> Unclassified 17. NUMBER OF PAGES <hr/> 18. PRICE					







**UNITED STATES
NUCLEAR REGULATORY COMMISSION
WASHINGTON, D.C. 20555**

OFFICIAL BUSINESS
PENALTY FOR PRIVATE USE, \$300

SPECIAL FOURTH-CLASS RATE
POSTAGE & FEES PAID
USNRC
WASH. D.C.
PERMIT No. G-67

NUREG/CR-4412

AN ASSESSMENT OF SAFETY MARGINS IN ZIRCALOY OXIDATION AND EMBRITTLEMENT
CRITERIA FOR ECCS ACCEPTANCE

APRIL 1986